UNIVERSITEIT VAN PRETORIA
UNIVERSITY OF PRETORIA
YUNIBESITHI YA PRETORIA

Solid-Liquid Mass Transfer in Trickle Bed Reactors

Rita Joubert

UNIVERSITEIT VAN PRETORIA
UNIVERSITY OF PRETORIA
YUNIBESITHI YA PRETORIA

Solid-Liquid Mass Transfer in Trickle Bed Reactors

by

Rita Joubert

A dissertation submitted in partial fulfilment of
the requirements for the degree

Master of Engineering (Chemical Engineering)

in the

Chemical Engineering
Faculty of Engineering, the Build Environment and Information Technology

University of Pretoria
Pretoria

13 February 2009

UNIVERSITEIT VAN PRETORIA
UNIVERSITY OF PRETORIA
YUNIBESITHI YA PRETORIA

Solid-Liquid Mass Transfer in Trickle Bed Reactors

Author: Rita Joubert

Supervisor: W. Nicol

Department: Department of Chemical Engineering
University of Pretoria

Degree: Master of Engineering (Chemical Engineering)

Abstract

Hydrodynamic multiplicity in the trickle flow, or low interaction, regime is a well documented phenomenon. Multiple hydrodynamic states are often presented in the form of hysteresis loops where the hydrodynamic parameter studied are shown as a function of the operating history of the bed, i.e. liquid and gas flow rates. In extreme cases the lower leg, representing an increase in liquid flow rate on a pre-wetted and drained bed, is commonly referred to as the Levec mode. The upper extreme, referred to as the Kan-liquid mode, represents a decrease in liquid flow rate after operation in the high interaction regime.

The many reported studies investigating liquid-solid mass transfer in trickle beds have generally used either the dissolution or electrochemical techniques. Numerous researchers have used their data to develop correlations predicting solid-liquid mass transfer coefficients. Most of these studies do not specify the multiplicity mode of operation. Only two studies (Sims et al. (1993) and Van der Merwe, Nicol & Al-Dahhan (2008)) use both the Levec and Kan-liquid operating modes. Both of these studies suggest that solid-liquid mass transfer also exhibit multiplicity behaviour although the trends suggested or speculated differ from each other. Sims et al. (1993) found that a Kan-liquid operated bed will outperform a Levec operated bed; however in contrast to this Van der Merwe et al. (2008) speculated that a Levec operated bed is better suited for liquid limited reactions due to enhanced liquid-solid mass transfer in the Levec mode as a result of faster interstitial velocity.

This study showed that solid-liquid mass transfer coefficients, measured with both the dissolution and electrochemical technique, show multiplicity behaviour. Two distinct operating regions were found, which corresponds to the Levec and Kan-liquid modes. Measurements taken using the electrochemical technique yielded solid-liquid mass transfer coefficients larger than those measured using the dissolution method. The experimental results agree with the trend found by Sims et al. (1993) but the mass transfer coefficients in this study were significantly lower. Additionally it was shown that the difference in mass transfer coefficients, in the two modes, cannot be explained by merely compensating for the differences in wetting efficiency and interstitial velocity, suggesting that the Levec mode has a larger percentage of stagnant or poorly irrigated zones. It was also shown that mass transfer coefficients measured at the top of the column is higher than those measured at the bottom, suggesting that the flow structure is changing as a function of axial length.

Lastly, with regards to electrochemical measurements of liquid-solid mass transfer, it was shown that measurements using a single particle electrode compared well to that of a multiple packing electrode.

Keywords: wetting efficiency, multiplicity, pre-wetting, solid-liquid mass transfer coefficient

Contents

Nomenclature

a - Effective area for mass transfer (cm^2/cm^3)

a_t - Total external surface area of particles per unit volume of empty tube (cm^2/cm^3)

a_s - Wetted active area of bed per unit bed volume (m^{-1})

a_v - Geometrical area per unit of bed volume (m^{-1}) $6(1-\varepsilon)/d_p$

A - Surface area of single particle (m^2)

A_c - Column cross sectional area (m^2)

A_e - Electrode area (cm^2)

c - Concentration ($gmol/cm^3$)

c^* - Concentration at particle surface ($gmol/cm^3$)

c^0 - Equilibrium concentration of hydrogen in alpha-methyl styrene (mol/cm^3)

C_p - Saturated dissolved oxygen concentration ($gmol/cm^3$)

c_S - Solubility of benzoic acid (g/ℓ)

D - Diffusivity (m^2/s)

D_{eff} - Effective diffusion coefficient in porous catalyst (cm^2/s)

d_p - Catalyst particle diameter (cm)

E_l - Liquid power dissipation parameter (W/kg liquid hold-up)

F - Faraday constant (C/mol)

g - Gravitational acceleration (kg/ms^2)

G - Gas flux (kg/m^2s)

h - Packing height (m)

H - Dynamic liquid hold-up (m^3/m^3)

I_{lim} - Limiting current (A)

j_D - Mass transfer factor

k - Mass transfer coefficient (m/s)

k_{lg} - Gas-liquid mass transfer coefficient (m/s)

k_{ls} - Solid-liquid mass transfer coefficient (m/s)

L - Liquid mass flux (kg/m^2s)

n - Number of active particles

n_e - Number of electrons involved in stoichiometric equation

N - Molar flux

P_w - Partial pressure of water vapour (Pa)

r - Rate of reaction (gmol/s.cm^3 of reactor volume)

S - Cross sectional area of empty tube (cm^2)

t - Temperature (°C)

T - Temperature (K)

U - Volumetric flow rate (m^3/s)

$u_{intrinsic}$ - Intrinsic liquid flow rate (mm/s)

V - Superficial velocity (m/s)

Dimensionless numbers

Ga - Galileo number (-) $\rho_l^2 g d_p^3 / \mu_l^2$

$Ga"$ - Modified Galileo number (-) $d_p^3 \rho_l \left(\rho_l g + \left(\frac{\Delta P}{z} \right) \right) / \mu_l^2$

Ko - Kolmogroff number (-) $E_l d_p^3 \rho_l^3 / \mu_l^3$

Re_l - Liquid Reynolds number (-) $\rho_l d_p V / \mu_l$

Sh - Sherwood number (-) $k_{ls} d_p / D$

Sc - Schmidt number (-) υ / D

Greek letters

ε - Void fraction in catalyst bed

ϕ - Fractional wetting of packing or electrode

η - Effectiveness factor

μ - Dynamic viscosity (Pa.s)

θ - Correlating variable (-)

ρ - Density (kg/m^3)

υ - Kinematic viscosity (m^2/s)

Subscripts

e - Effluent from bed

f - Feed to bed

g - Gas

l - Liquid

s - Solid

Chapter 1. Introduction

Trickle bed reactors are packed beds with co-current down flow of the gaseous and liquid reagents and are widely encountered in the petrochemical and associated industries. Designing these reactors requires knowledge of the resistance to absorption of the gaseous component into the liquid phase and the transfer of the reacting species through the liquid-solid film to the catalyst.

It has been shown that hydrodynamics in the trickle flow, or low interaction, regime is not uniquely determined by the operating conditions. The existence of multiple hydrodynamic states complicates the prediction of trickle bed reactor performance. Multiple states are presented in the form of hysteresis loops where the hydrodynamic parameter studied is shown as a function of the operating history of the bed, i.e. the liquid and gas flow rates (Levec, Grosser & Carbonell, 1988; Loudon, Van der Merwe & Nicol, 2006). In extreme cases the lower leg represents parameters in the Levec operating mode, an increasing flow rate, and the upper leg represents parameters in the Kan-liquid operating mode, decreasing flow rate after operating in the pulsing or high interaction regime. These modes can also be reached by simply pre-wetting the bed with the applicable pre-wetting procedure.

There are many reported studies investigating liquid-solid mass transfer (LSMT) in trickle beds (examples are: Rao & Drinkenburg, 1985; Satterfield, Van Eek & Bliss, 1978; Al-Dahhan, High-Fill & Tee Ong, 2000). These studies have generally used one of two methods, dissolution or electrochemical, although various other techniques such as chemical reaction and absorption have been proposed. Numerous studies have been done to find correlations predicting solid-liquid mass transfer coefficients. These correlations are based on studies with a large variation in experimental data and cannot be compared to one another as most researchers do not state which preconditioning methods they used thus resulting in different hydrodynamic states.

The only studies investigating both of these operating modes are that of Sims, Schultz & Luss (1993) and Van der Merwe et al. (2008). Sims et al. (1993) used an electrochemical method and found that the mass transfer in a Kan-liquid operated bed is higher than that measured in a Levec operated bed. Opposed to this Van der Merwe et al. (2008), using a chemical reaction method (the hydrogenation of alpha-methyl-styrene) explained his reaction measurements by speculating that a Levec operated bed is better suited for liquid limited reactions. He attributes this counter-intuitive behaviour to higher interstitial velocities observed in the Levec mode.

The aim of this study was to quantify the differences in solid-liquid mass transfer in the Levec and Kan-liquid operating modes. This was done through the use of three techniques, two electrochemical and one dissolution technique. The effect of using a single or multiple packing electrode was evaluated using a well studied electrochemical method. These results were further compared to results obtained with the dissolution technique. The influence of column height, hold-up and wetting efficiency on solid-liquid mass transfer coefficients were also investigated.

Chapter 2. Literature Study

2.1 Measuring techniques for liquid-solid mass transfer in trickle bed reactors

A Variety of studies have been done to determine solid-liquid mass transfer coefficients. The majority of the studies focused on the electrochemical and dissolution techniques; however other methods such as chemical reaction (Morita & Smith, 1976) and activated carbon absorption (Tan & Smith, 1982) have also been used.

Local instantaneous mass transfer coefficients and local mass transfer coefficient fluctuations can be inferred from measuring the current in an electrochemical system. Overall mass transfer coefficients can be measured using absorption, chemical reaction or a dissolution technique.

In this section a brief overview of the experimental techniques are given. Even though previous studies are mentioned in the table above only a select number of references are summarised in below in section 2.2.

2.1.1 Electrochemical technique

This method is employed to measure the local instantaneous solid-liquid mass transfer coefficient at a certain position within the bed. The gas and liquid phases are fed co-currently up or down the reactor. The liquid phase consists of a solvent, an electrolyte and a supporting electrolyte, which is added to reduce the migration current.

A cathode, with the same size and geometry as the inert packing, is placed at a certain radial and axial position within the bed. An anode, with surface area greater than the cathode, is placed down stream of the cathode or at the outlet of the reactor. A negative voltage is applied to the cathode which drives the reaction at the electrode surface. The current produced by the transfer of electrons flows

through the electrochemical cell. The applied voltage is controlled so that the reaction at the electrode is liquid diffusion limited.

Figure 1 shows a plot of cell current as a function of applied voltage for two systems. Position B shows the plateau representing the operating condition under which the electrode is polarized. Since an increase in applied voltage does not lead to an increase in current the overall reaction rate is dominated by solid-liquid mass transfer. The portion of the curve represented by A indicates conditions where the kinetics is slower than the mass transfer, and the reaction is said to be kinetically limited. Operating conditions in portion C is typically due to additional reaction, such as the hydrolysis of water.

If the onset of additional reactions occurs at a low enough voltage the electrode may not polarize. In this case the kinetics is so slow or the solid-liquid mass transfer so fast that a polarization plateau may not exist, this is illustrated by the dashed line D.

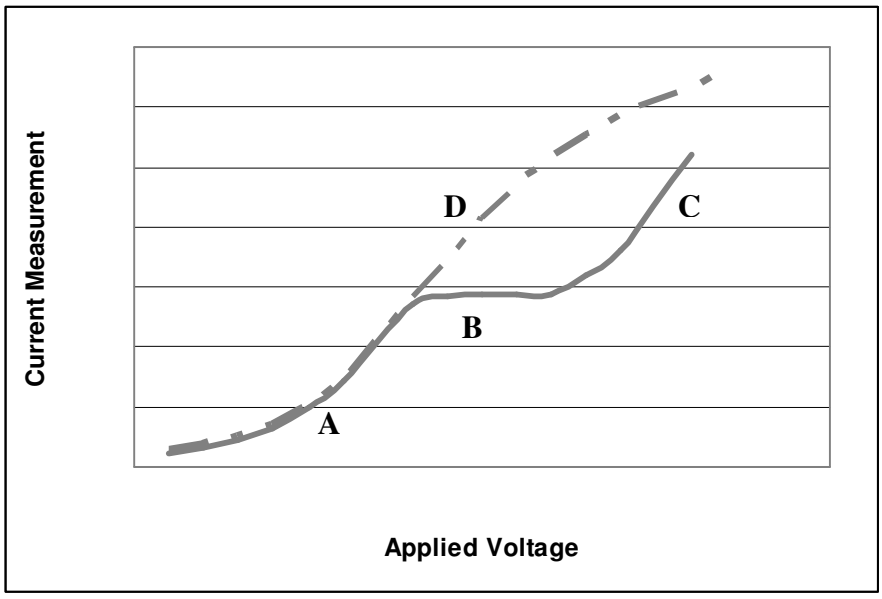

Figure 1: Electrode polarization (taken from Hanratty & Campbell, 1983)

The current produced by the electrochemical reaction is measured and can be related to the mass transfer coefficient by equation 1 or to the molar flux using equation 2 (Hanratty & Campbell, 1983).

$$I_{\lim} = Fk_{ls}A_e c \quad \text{(eq 1)}$$

$$I_{\lim} = n_e F A_e N \quad \text{(eq 2)}$$

The majority of investigations, taking into account the solvent and electrolyte selection criteria suggested by Latifi, Laurent & Storck (1988) and Hanratty & Campbell (1983), are based on the potassium ferricyanide $(K_3Fe(CN)_6)$ – potassium ferrocyanide $(K_4Fe(CN)_6)$ system using a single packed electrode. However Delaunay et al. (1982) and Latifi et al. (1988) used an electrode consisting of multiple active spheres (composite packed electrode) to determine the overall mass transfer coefficient.

2.1.2 Dissolution technique

This method has predominantly been used at atmospheric conditions to measure the overall solid-liquid mass transfer coefficient in a packed bed with two phase flow. Active particles are made by casting particles or by coating kernel particle with a sparingly soluble solid; this prevents large changes in bed characteristics. Different types of solid material have been used, such as benzoic acid, a mixture of benzoic acid and a fluorescent dye (Rhodamine B), naphthalene and β-napthal. (Al-Dahhan, High-Fill & Tee Ong, 2000)

Investigators have either used short beds of active particles or longer beds with a section of active particles to avoid saturation of the liquid effluent. The active particles can also be dispersed throughout the bed in an amount equal to a short section. The saturation level of the effluent should not exceed 70% as this limits the experimental accuracy.

A variety of measuring techniques have been employed to measure the concentration of dissolved material in the liquid effluent. Depending on the dissolving material, researchers have suggested the use of a fluorometer, UV spectrometer or titration with $NaOH$. Using a plug flow assumption Goto et al. (1975) stated that the inlet and outlet concentrations can be related by equation 3.

$$k_{ls}a = \frac{U_L}{a_S h}\ln\left[\frac{c_S - c_f}{c_S - c_e}\right] \qquad \text{(eq 3)}$$

2.1.3 Chemical reaction

Hydration and hydrogenation reactions are commonly used as the rate controlling step can be altered, by changing the superficial liquid velocity, so that the overall reaction rate is controlled by the rate of diffusion of the liquid reagent through the liquid boundary layer to the catalyst surface.

Gas and liquid reagents flow through a bed of catalyst particles. The reagents are converted to products at slightly elevated temperatures (up to 50°C). This ensures a vapour pressure low enough to keep the products in the liquid phase. The solid-liquid mass transfer coefficient can be determined by measuring the concentration of the reaction products in the liquid effluent.

Satterfield et al. (1969) proposed that the magnitude of the resistance in the liquid film can be determined by equating the flux through the liquid film to the reaction rate. Both the flux and the reaction rate are taken per unit of outside surface area of catalyst. The correlation used for this computation is given here as equation 4.

$$k_{ls}\left(c^0 - c^*\right) = \frac{2\phi D_{eff} c^*}{d_p}\left(\frac{1}{\tanh\phi} - \frac{1}{\phi}\right) \qquad \text{(eq 4)}$$

2.1.4 Absorption

The gas and liquid phase, an aqueous solution usually containing benzaldehyde, flows co-currently through a bed of granular activated carbon particles. The dynamic absorption is inferred by measuring the concentration of benzaldehyde in the liquid effluent. Intraparticle diffusion effects, which may affect the effluent concentration, can be eliminated by extrapolating the absorption data to zero time.

2.1.5 Advantages and disadvantages of measuring techniques

The electrochemical method is one of the most widely used techniques for the determination of solid-liquid mass transfer coefficients as it is the only method where the state of the transfer unit remains unchanged. This technique is also the only technique that measures local mass transfer coefficients and can therefore be used, when operating in the high interaction regime, to compare the mass transfer in a liquid rich slug to that in a gas rich slug. However a reduction in liquid conductibility as a result of degradation of electrolyte due to prolonged light exposure, can lead to local and temporal variation in mass transfer coefficients

Overall mass transfer coefficients are measured when the dissolution, chemical reaction or absorption techniques are used. These techniques are said to give more repeatable results when operating in the LIR as wetting efficiencies of the particles are averaged. When using the electrochemical technique, with a single packing electrode, the wetting efficiency of the electrode may not be equal to that of the previous run and either lower or higher coefficients may be recorded.

When using the dissolution technique, some researchers, prefer using coated particles, even though they risk dissolving all the material before the end of an experiment, as oppose to using cast particles which can lead to changes in bed characteristics.

The use of chemical reactions and absorption techniques make it possible to operate the packed bed as a differential reactor. Experimental errors is reduced as the surface area per catalyst weight is provided by the manufacturer and not calculated. Possible catalyst poisoning and deactivation will not necessarily be observed and can lead to wrong interpretation of the experimental results.

2.2 Prominent studies on solid-liquid mass transfer in packed bed reactors

Liquid-solid mass transfer coefficients are one of the most important parameters for the design, scale-up and performance characterization of packed beds. Various studies have been done to determine the mass transfer in a bed and many correlations have been suggested to predict solid-liquid mass transfer coefficients for different systems. Most of these studies, with exception to the research groups in Nance, Washington University and the University of Twente, were done under atmospheric conditions (Al-Dahhan *et al.*, 1997).

The table below show some of the previous studies on this subject. Techniques used and operating regimes (flooded, trickle, transition, pulse, dispersed bubble flow) are indicated; other significant findings (i.e. where height and radial position of electrode were studied or where experiments were performed at elevated temperature and/or pressure) are also included. The forth column indicates whether the researchers suggested a predictive correlation. The preconditioning methods used are not given as numerous researchers did not report their mode of operation.

Table 1: Solid-liquid mass transfer studies

Reference	Technique used	Operating regime	Correlation suggested	Other findings
Al-Dahhan et al. (2000)	Dissolution of naphthalene	none specified	N	-
Bartelmus (1989)	Electrochemical	flooded, trickle & pulse	Y	-
Barthole (1982)	Electrochemical	flooded	Y	-
Boelhouwer (2001)	Electrochemical	trickle & pulse	Y	-
Burghardt et al. (1995)	Electrochemical	pulse	Y	-
Chou et al. (1979)	Electrochemical	trickle & pulse	Y	-
Delaunay et al. (1982)	Electrochemical	trickle & pulse	Y	-
Dharwadkar & Sylvester (1977)	-	gas continuous, transition, pulse and dispersed bubble	Y	correlating previously published data
Goto et al. (1975)	Dissolution of naphthalene	trickle	N	-

Herskowitz et al. (1979)	Hydrogenation of alpha-methylstyrene	flooded & trickle	Y	-
Hirose et al. (1976)	Dissolution of benzoic acid	dispersed bubble & pulse	Y	-
Jolls & Hanratty (1969)	Electrochemical	trickle & pulse	Y	-
Lakota & Levec (1990)	Dissolution of naphthalene	trickle & pulse	Y	-
Latifi et al. (1988)	Electrochemical	flooded & trickle	Y	-
Lemay et al. (1975)	Dissolution of benzoic acid	pulse	Y	-
Mochizuki et al. (1976)	Hydrogenation of phenylacetate and styrene	none specified	Y	differential reactor
Morita & Smith (1978)	Hydrogenation of alpha-methylstyrene	flooded & trickle	Y	-
Rao & Drinkenburg (1985)	Electrochemical	trickle & pulse	Y	-
Reuther et al. (1980)	Dissolution of benzoic acid	gas continuous, transition, pulse and dispersed bubble	Y	-
Satterfield et al. (1978)	Dissolution of benzoic acid	trickle & pulse	Y	-
Sims et al. (1993)	Electrochemical	trickle & pulse	Y	multiplicity in trickle flow
Specchia et al. (1978)	Dissolution of benzoic acid	flooded & trickle	Y	-
Sylvester & Pitayagilsarn (1975)	Dissolution of benzoic acid	gas continuous, transition, pulse	Y	-
Tan & Smith (1980)	Dissolution of benzaldehyde	trickle	Y	-
Trivizidakis & Karabelas (2006)	Electrochemical	flooded, trickle & pulse	Y	effect of bed depth
Van der Merwe (2008)	Hydrogenation of alpha-methylstyrene	trickle	N	multiplicity in trickle flow
Van Krevelen & Krekels (1948)	Electrochemical	trickle	Y	-
Wilson & Geakoplis (1966)	Dissolution of benzoic acid and naphthol	trickle & pulse	Y	-

Various researchers have published their mass transfer data obtained using the techniques discussed in section 2.1. A short overview of widely referenced studies is given below in chronological order. It should be noted that most of the researchers found that the Sherwood number has a dependence on the liquid Reynolds number close to the power of 0.5 suggested by the boundary layer theory.

Jolls & Hanratty (1969)

The bed, used for electrochemical experiments, consisted of a 60 inch length of 12 inch diameter glass pipe, packed with 1 inch glass spheres. A test sphere, located 7 to 8 inches from the top of the column acted as the cathode and a section of nickel-coated pipe, located outside the column, was used for the anode.

The electrolyte, aqueous solution of equimolar concentrations (10^{-2}M) of $K_4Fe(CN)_6$ and $K_3Fe(CN)_6$ and 1M sodium hydroxide ($NaOH$), was pumped from the bottom of the reactor which ensured complete wetting of the electrode.

They found that their results, for a given packing arrangement, were reproducible and showed little to no scattering for Re >35. They correlated their data for different ranges of Re using equation 5. Average values of the variables for the different ranges are given in table 2. The effect of Reynolds number on the mass transfer coefficient to a sphere in a packed bed of inert spheres or in a bed of active spheres indicated a slightly larger power of the Reynolds number than the 0.5 predicted by the boundary layer theory.

$$ShSc^{-1/3} = A\,\mathrm{Re}^{n} \qquad \text{(eq 5)}$$

Table 2: Variables for substitution in equation 5 at different ranges of Re

Reynolds number	A	N
Re<35	1.64	0.60
35<Re<140	1.44	0.58
140<Re<1120	1.59	0.56
Re>1120	6.4	0.50

Mochizuki & Matsui (1976)

These researchers used the hydrogenation of phenylacetate and styrene to quantify the solid-liquid mass transfer coefficient. They used an up-flow arrangement as this gave afar better selectivity compared to a down-flow arrangement. They found that equation 6 and 7 best fit the data for single phase and two phase co-current flow.

$$Sh' = 0.75\,\mathrm{Re}_l^{1/2}\,Sc^{1/3} \qquad \text{(eq 6)}$$

$$\frac{Sh}{Sh'} = \left(1 + 4\frac{\mathrm{Re}_g^{0.55}}{\mathrm{Re}_l^{0.7}}\right)Sc^{1/3} \qquad \text{(eq 7)}$$

Sylvester & Pitayagulsarn (1975)

Air and water was co-currently fed to the top of a packed column and the dissolution of benzoic acid from cast spheres was measured. Samples of the effluent were analysed by titrating with a $NaOH$ (0.01N) solution to a phenolphthalein end point. The correlation they suggested (eq 8) pertains to the gas continuous, transition and pulse flow regimes.

$$k_{ls}a = 1.634 * 10^{-4}\left[L^{-0.78}\left(1 - \frac{\varepsilon^y}{1+\varepsilon^y}\right)\right]G^{0.38} \qquad \text{(eq 8)}$$

$$y = 4L/6350 \qquad \text{(eq 9)}$$

Hirose, Mori & Sato (1976)

Two systems were used to determine the solid-liquid mass transfer coefficient. System A employed the dissolution of benzoic acid spheres, made by coating kernel particles with molten benzoic acid. In system B a diffusion limited redox reaction, between metallic copper and dichromate ions in sulphuric acid solution, was used. System A was not used at low liquid flow rates to avoid channelling due to poor wettability of benzoic acid and system B was not used at high liquid flow rates due to difficulties handling large amounts of corrosive materials.

They found that the different techniques yield similar mass transfer coefficients for measurements taken when operating in the transition regime. They reported a smooth transition between the regimes. Results in the trickle flow regime was correlated with equation 10, equation 8 suggested by Sylvester & Pitayagulsarn (1975) was used to model the results obtained in the pulse flow regime.

$$\phi Sh = 1.56\,\mathrm{Re}_l^{1/2}\,Sc^{1/3} \qquad \text{(eq 10)}$$

Satterfield, Van Eek & Bliss (1978)

In this work mass transfer coefficients were determined by measuring the rate of dissolution of cylindrical benzoic acid particles into distilled water. A wide range of flow conditions were covered, from single phase liquid flow to pulsing gas-liquid flow.

In the trickle flow regime, characterised by incomplete wetting, the results showed an average absolute percentage deviation of 10.8%. The data obtained in the pulse flow regime, generally accepted as a perfectly wetted condition, showed an average absolute percentage deviation of 7.2%. The correlations suggested for use in the different flow regimes are given below.

$$\phi Sh = 0.815\,\mathrm{Re}_l^{0.822}\,Sc^{1/3} \qquad \text{(eq 11)}$$

$$\phi Sh = 0.334\,Ko^{0.202}\,Sc^{1/3} \qquad \text{(eq 12)}$$

Specchia, Baldi & Gianetto (1978)

The volumetric solid-liquid mass transfer coefficients in co-current downward and upward two-phase flow were determined by dissolution of benzoic acid cylinders. Results obtained in the liquid full regime (up-flow of liquid) showed a mean relative quadratic error of 4.7% and is well described by equation 13. Trickle flow, with single phase downward liquid flow and two phase flow with a gas flow rate up to 1.56m/s, data gave a mean relative quadratic error of 17.9% and 7.6% respectively. The experimental data can be correlated with equations 14 and 15.

$$Sh' = \left(2.14\,\mathrm{Re}_l^{\,0.5} + 0.990\right) Sc^{1/3} \qquad \text{(eq 13)}$$

$$Sh' = \left(10.8(1-\varepsilon)\,\mathrm{Re}_l^{\,0.5}\right) Sc^{1/3} \qquad \text{(eq 14)}$$

$$\ln\frac{Sh}{Sh'} = 0.48\ln\left(\frac{\mathrm{Re}_g}{\mathrm{Re}_l}10^2\right) - 0.30\left[\ln\left(\frac{\mathrm{Re}_g}{\mathrm{Re}_l}\right)10^2\right]^2 - 0.30 \qquad \text{(eq 15)}$$

Chou, Worley & Luss (1979)

A single nickel cathode in a bed of alumina spheres were used in these electrochemical experiments. The electrolytic solution contained equimolar amounts (0.008M) of $K_4Fe(CN)_6$ and $K_3Fe(CN)_6$ and roughly 0.78M $NaOH$.

In the gas continuous regime a large scatter of data was obtained with electrodes at different position within the bed, however time averaged data obtained in the pulse regime was independent of the electrode position. As a result of the large scatter in data they did not suggest a correlation for data in the gas-continuous regime, however they suggested that mass transfer coefficients, for $40<Re_g<300$ and $50<Re_l<140$, can be predicted by equation 16. The average deviation of the experimental data from the suggested correlation was 4.7%.

$$\phi Sh = \frac{0.72\,\mathrm{Re}_l^{\,0.54}\,\mathrm{Re}_g^{\,0.16}\,Sc^{1/3}}{\varepsilon} \qquad \text{(eq 16)}$$

Reuther, Yang & Hayduk (1980)

The packed bed used for dissolution experiments was divided into three sections, two inert sections and an active section in a central horizontal portion of the bed. The active section consisted of berl saddles coated with a 1% (in weight) mixture of rhodamine B and benzoic acid. The addition of a dye made it possible to use a fluorometer for continuous measurement of the effluent concentration.

The gas and liquid superficial velocities ensured operation in all four the major flow regimes. The mass transfer rates were reproducible within 8% in all the flow regimes except for the gas continuous regime for which the reproducibility was

11%. They suggested correlations (equation 17, 18 & 19) for mass transfer coefficients in the gas continuous (Re_l<55), transition (55<Re_l<100) and pulse and dispersed bubble flow (Re_l>100) regimes.

$$\phi Sh = \frac{0.0819\,\mathrm{Re}_l^{\,0.777}\,Sc^{1/3}}{\varepsilon} \qquad \text{(eq 17)}$$

$$\phi Sh = \frac{0.00437\,\mathrm{Re}_l^{\,1.517}\,Sc^{1/3}}{\varepsilon} \qquad \text{(eq 18)}$$

$$\phi Sh = \frac{0.68\,\mathrm{Re}_l^{\,0.416}\,Sc^{1/3}}{\varepsilon} \qquad \text{(eq 19)}$$

Rao & Drinkenburg (1985)

Local instantaneous solid-liquid mass transfer coefficients were measured using the electrochemical technique. The liquid phase, a solution of 0.006M $K_3Fe(CN)_6$, 0.05M $K_4Fe(CN)_6$ and 1M $NaOH$, and the gas phase, air, was co-currently fed to the top of the packed bed of cylindrical particles. The mass transfer to a single particle in the bed was measured under diffusion limited conditions.

A wide range of liquid and gas flow rates were used to cover the trickle, ripple and pulse flow regimes. The mass transfer coefficients for trickle and ripple flow can be represented by equation 20, obtained with a linear least-squares regression of experimental results, and showed a root mean square deviation of 6.5% of the experimental data. Pulse flow data was evaluated using limited current measurements as well as an energy dissipation model. This data is well represented by equation 21 and 22, showing a root mean square deviation of 7.8%.

$$\phi Sh = 0.24\,\mathrm{Re}_l^{\,0.75}\,Sc^{1/3} \qquad \text{(eq 20)}$$

$$\phi Sh = \frac{0.77\,\mathrm{Re}_l^{\,0.45}\,\mathrm{Re}_g^{\,0.223}\,Sc^{1/3}}{\varepsilon} \qquad \text{(eq 21)}$$

$$\phi Sh = 0.71\,Ko^{0.21}\,Sc^{1/3} \qquad \text{(eq 22)}$$

Latifi, Laurent & Storck (1988)

An electrochemical reaction, the reduction of DMSO (dimethylsulphoxide), at the cathode (a 7.5cm section of the reactor packed with platinum coated spheres) was used to quantify solid-liquid mass transfer coefficients.

The overall mass transfer coefficient between the flowing liquid and the packing particles, the cathode, was deduced from the limiting current intensity measurements. The mass transfer factor calculated from the data obtained in the liquid-full operating mode is well represented by the correlation suggested by Satterfield & Resnick (1954), given as equation 23 below.

$$j_D = 0.667\,\mathrm{Re}_l^{-0.34} \qquad \text{(eq 23)}$$

Lakota & Levec (1990)

These researchers measured the dissolution of naphthalene into water. They manufactured their packing particles by pressing a mixture of naphthalene, stearate and talc into cylindrical particles. The bed was preconditioned using the Kan-liquid pre-wetting procedure. After pre=treatment the gas and liquid were co-currently passed through the bed. Gas flow was kept constant while the liquid flow rate was incrementally increased over a range of operating points which span the low interaction and high interaction regimes. They correlated the data, for the entire range of operating conditions, by equation 24 which showed a mean relative deviation of 7.2% from the experimental results.

$$Sh = 0.487\,\mathrm{Re}_l^{0.495}\,Sc^{1/3} \qquad \text{(eq 24)}$$

Sims, Schultz & Luss (1993)

The electrolytic solution of 0.01M $K_3Fe(CN)_6$, 0.0125M $K_4Fe(CN)_6$ and 1M $NaOH$, was used in their electrochemical experiments. Cathode pellets were made from solid nickel rod and placed at one axial position, at different radial positions, within a bed packed with cylindrical solid fluoropolymer extrudates. Gas and liquid were co-currently fed to the top of the column. Gas flow was kept constant

while the liquid flow rate was first increased from the LIR to the HIR and then decreased from the HIR back to the LIR.

The data clearly indicated that the solid-liquid mass transfer coefficient exhibited hysteretic behaviour in the low interaction regime (shown in figure 2 below). The experimental data obtained in the pulsing regime can be correlated using the equation below.

$$\phi Sh = 5.4\,\mathrm{Re}_l^{0.44}\,Sc^{1/3} \qquad \text{(eq 25)}$$

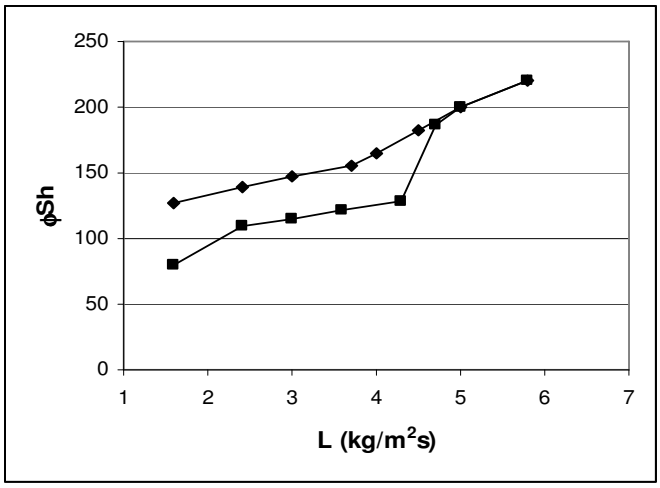

Figure 2: Hysteretic behaviour of the Sherwood number with a change in liquid flow rate (taken from Sims et al., 1993)

Trivizidakis & Karabelas (2006)

These researchers used the well known potassium ferri- ferrocyanide system in their electrochemical study. Ten uniform spherical and fourteen cylindrical nickel particles were used as cathodes. These electrodes were placed at various axial and radial positions throughout the bed.

The data obtained with cylindrical extrudates under steady trickling flow were significantly lower, by a factor of 3, than the predictions from the correlations by Satterfield et al. (1978) and by Rao & Drinkenburg (1985). Experimental results obtained in the pulsing regime, for spherical particles, were relatively close to the prediction by Rao & Drinkenburg (1985) and in even closer agreement with the

data of Sylvester & Pitayagulsarn (1975). The present global-average values for induced pulsing can be correlated by equation 26.

$$Sh = 0.35\,\mathrm{Re}_l^{0.6}\,Sc^{1/3} \qquad \text{(eq 26)}$$

2.3 Comparison of results from prominent solid-liquid mass transfer studies

Figure 3 shows previously suggested correlations, which simplify the comparison of data obtained with the use of different techniques. These correlations are shown at the liquid Reynolds numbers where they were developed. The gas Reynolds numbers are not included as it is generally accepted that its affect on Sherwood numbers are minimal for operation in the LIR. It is clear that the electrochemical technique tend to result in higher Sherwood numbers. An exception to this is the work done by Trivizidakis (2006) that resulted in mass transfer values similar to that measured using the dissolution technique. It is interesting to note that the both the data by Levec & Lakota (1990) and Trivizidakis (2006) was obtained in a Kan-liquid operated bed.

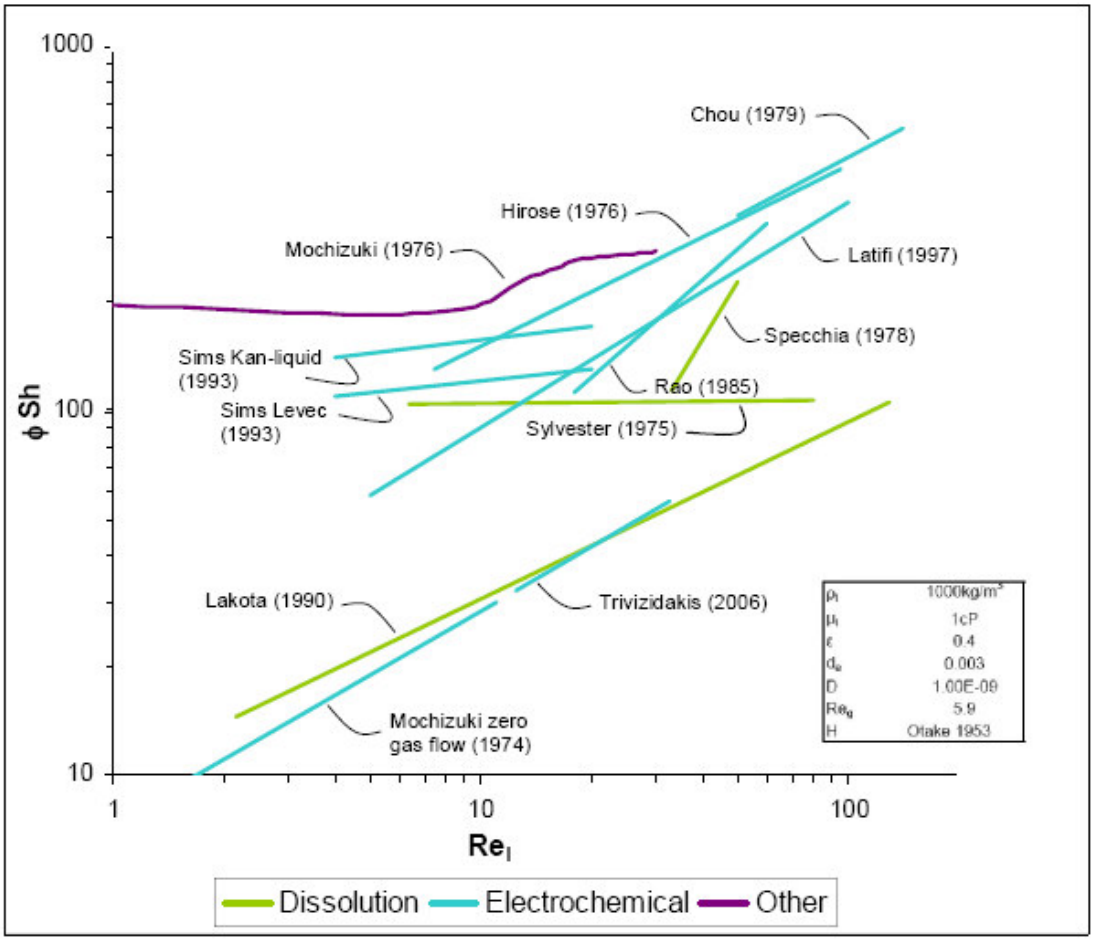

Figure 3: Comparison of suggested correlations (d_p=0.003m, V_g=0.03m/s)

2.4 Solid-liquid mass transfer multiplicity

Hydrodynamic parameters (such as pressure drop, liquid hold-up and mass transfer) are related to solid-liquid-gas contacting effectiveness and the operational efficiency of the reactor. These parameters are path variables, which greatly complicate the mathematical description and performance evaluation of trickle-bed reactors. The existence of multiple hydrodynamic states is often referred to as hydrodynamic multiplicity (Van der Merwe, 2008).

A major concept in previous experimental studies is hysteresis loops. These loops involve the increase and then decrease of some operating variable (for example gas – or liquid flow rate). Maiti et al. (2006) recently reviewed and

summarised earlier work done on hysteresis loops. Van der Merwe (2008) used figure 4 and the description below as an example of how pressure drop hysteresis loops are obtained.

Starting from a low (or zero) liquid velocity, the liquid flow rate is incrementally increased. The pressure drop increases accordingly (following the blue line) and reaches points A, B and C at liquid velocities $u_{L,1}$, $u_{L,2}$ and $u_{L,pulse}$ respectively. Further increasing the velocity beyond the trickle-to-pulse flow boundary also increases the pressure drop (following the grey line). When the velocity is decreased, the pressure drop decreases following the same path (grey) as before until $u_{L,pulse}$ is reached. A further decrease in u_L will mean a reduction in the pressure drop along the black line (which may be several times higher than the corresponding values on the increasing blue leg). At $u_{L,1}$ the pressure drop reaches point D. Note that all the operating conditions at this point are identical to those at point A – the only difference between the upper and lower legs is the operating history of the bed.

If the liquid velocity is increased from zero to $u_{L,2}$ (which is lower than $u_{L,pulse}$) and then decreased, the pressure drop follows the dashed line and reaches a point E at $u_{L,1}$. This means that at $u_{L,1}$, any pressure drop between that of points A and D can be attained depending on the highest liquid flow velocity reached. Alternatively Levec pre-wetting (see table 2) can be used to achieve operating points on the lower leg and Kan-liquid pre-wetting can be used to achieve operating points on the top leg.

Table 3: Limiting cases of hydrodynamic multiplicity (taken from Van der Merwe, 2008)

Name	Description
Levec- pre-wetted-mode	Dry particles are loaded into a dry bed. The reactors is completely flooded for several hours and then drained under gravity until only the residual liquid hold-up remains. The liquid and the gas flow rates are increased from zero to the operating values.
Kan-Liquid-pre-wetted-mode	Dry particles are loaded into a dry bed. The reactor is flooded for several hours and then drained. The gas flow is introduced at the operating velocity and kept constant while the liquid velocity is increased from zero to a value greater than the pulsing velocity. The pulsing regime is maintained for several seconds, the liquid flow rate is then reduced to the operating velocity.

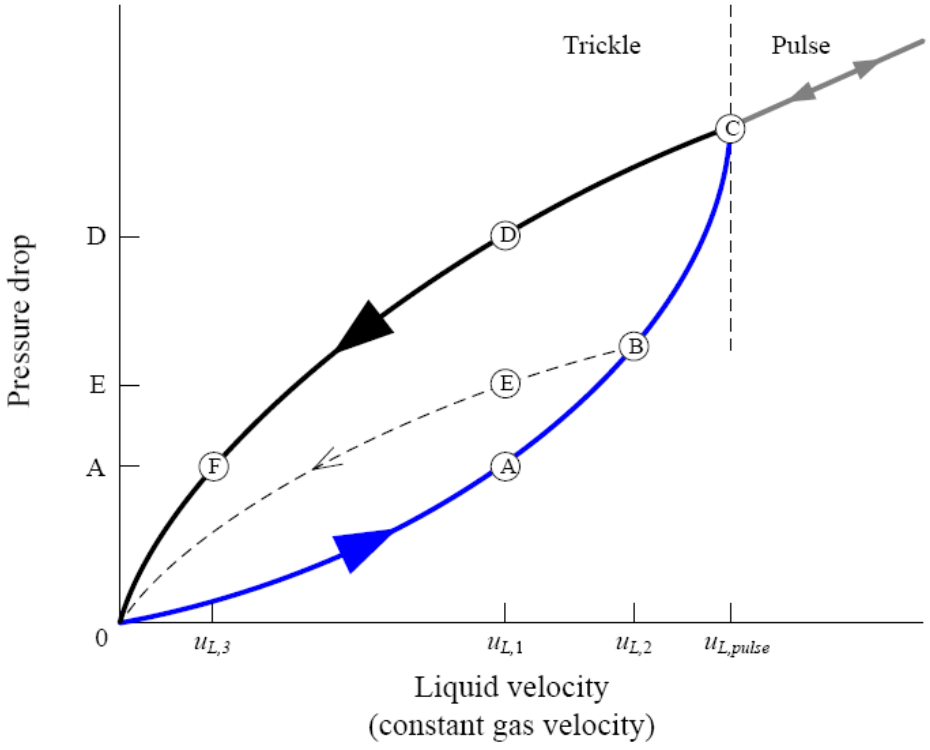

Figure 4: A schematic hysteresis loop (Van der Merwe, 2008)

Two previous studies (Sims et al. (1993) and Van der Merwe et al. (2008)) showed that solid-liquid mass transfer coefficients also exhibit hysteretic behaviour. However the results of these studies are quite different. Sims et al. (1993) found, using the electrochemical method, that a Kan-liquid pre-wetted bed outperforms a Levec pre-wetted bed. Van der Merwe et al. (2008) used the hydrogen of alpha-methyl-styrene and inferred solid-liquid mass transfer, this led to the conclusion that a Levec pre-wetted bed outperforms a Kan-liquid wetted bed under liquid limited conditions.

Chapter 3. Experimental

3.1 Trickle flow experimental unit

The experimental setup was designed to enable dynamic monitoring of the pressure drop and the gas-liquid mass transfer coefficients. All experiments were performed at atmospheric temperature and pressure which allowed for comparison of the experimental results with published data. A schematic drawing of the setup is shown in figure 5.

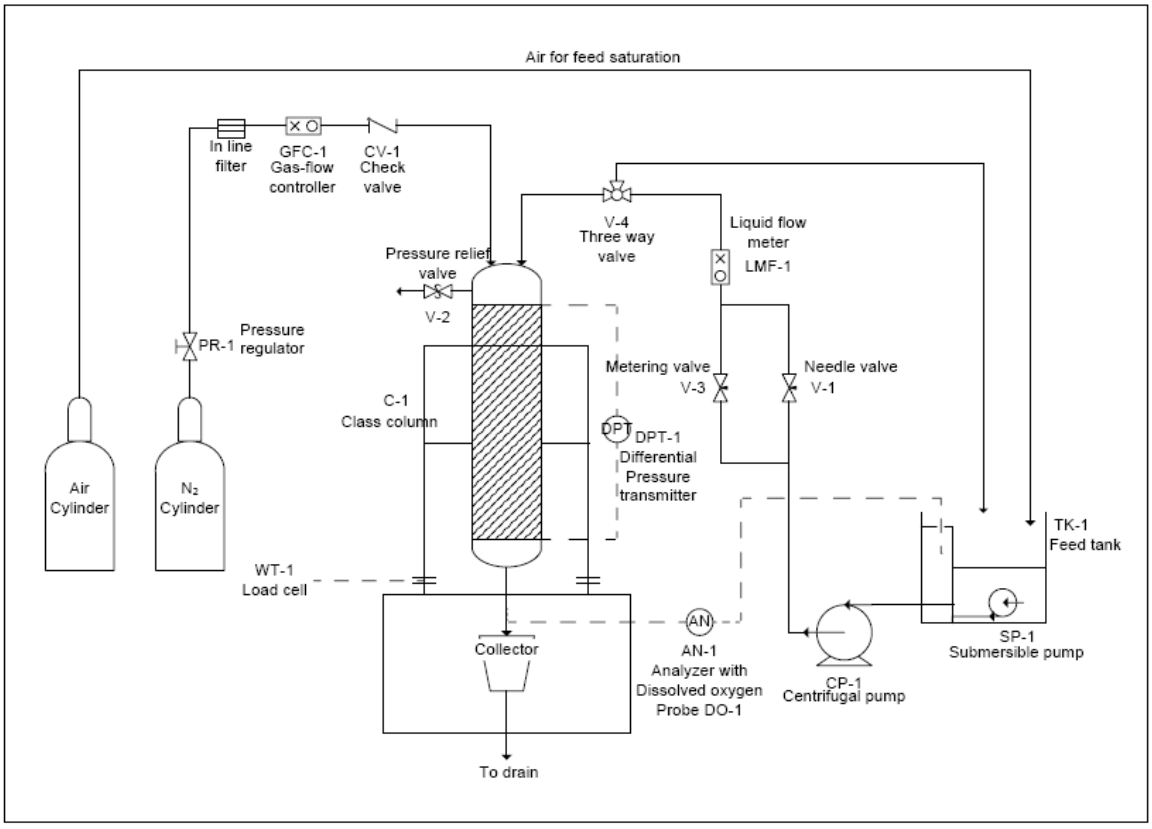

Figure 5: Experimental Setup

The reactor was a 1m long glass column with internal diameter of 63mm. The column was designed with a pressure release valve (V-2), which provides an outlet for gas when the column is flooded. The feed tank (TK-1) was filled with the required liquid and pre-saturated with oxygen by mixing the liquid with air. A

weir and submersible pump (SP-1) was used to ensure a constant pressure head.

The liquid flow rate was measured by an Electromagnetic Flow Measuring System (the PROline promag10H from Endress + Hauser), which has an accuracy of 1.5% of the rate when the flow is between 0.2 and 1ℓ/min and an accuracy of 0.5% of the rate when the flow is above 1ℓ/min. The flow was adjusted with the use of two parallel valves. A needle valve (V-1) was used to control the bulk flow rate and a meter valve (V-3) was used for fine tuning. A three way valve (V-4) was used to recycle the liquid while the column was drained. The gas flow rate was controlled with a Brooks Smart Mass Flow Model 5851S. The range of this flow meter is 0 – 100ℓ/min, it is calibrated for nitrogen and has an accuracy of 0.7% of the range.

Gas and liquid were fed into the column through a distributor. A schematic drawing of the distributor used in all the experiments is shown in figure 6. The holes in the distributor are 0.5mm in diameter and are spaced 8mm apart in a square pitch arrangement, with a drip-point density of 16000points/m^2. This drip point density conforms to the minimum density of 5000points/m^2 suggested by Burghardt et al. (1995). The cap contains three 0.25” stainless steel tubes through which the gas is fed into the column. This arrangement ensured that liquid distribution stayed uniform even at high gas flow rates.

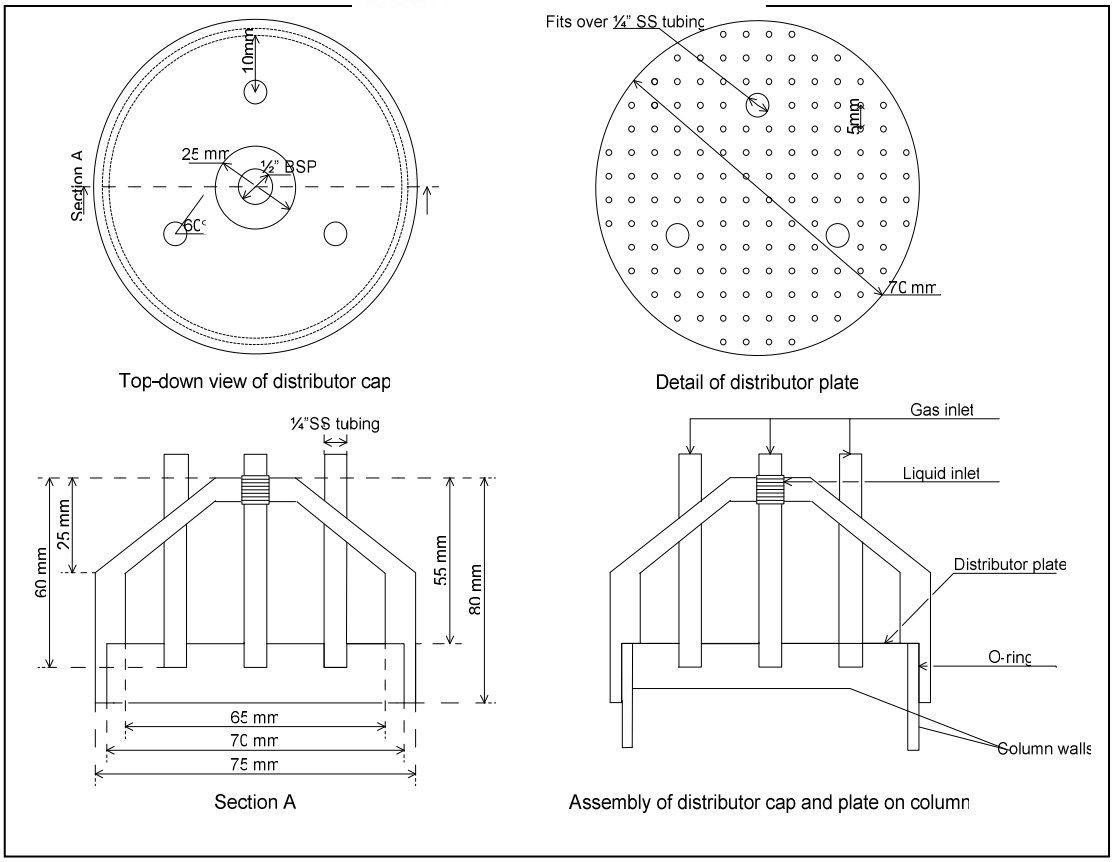

Figure 6: Schematic diagram of the gas-liquid distributor used

The packing particles used was 3mm glass beads, which according to Tsochatzidis et al. (2002) and Gianetto et al. (1978) result in more uniform distribution than other types of packing or spherical packing with a larger diameter. A metal sieve (the holes are 2.5mm) adequately supported the packing and did not result in the build-up of a liquid head, which may alter pressure drop readings. The column was packed to a height of 85cm.

A load cell (WT-1), a Rosemount Model 3051CD Pressure Transmitter (DPT-1) and a Dissolved Oxygen Sensor, 499ADO from Rosemount Analytical (AN-1), enabled the measuring of the bed porosity, pressure drop and gas–liquid mass transfer coefficients. The packed bed was loaded and mounted on the load cell stand and the mass of the packing was recorded. From this the bed porosity was calculated, as shown in equation 27. The average porosity for all the experiments were approximately 0.4.

$$\varepsilon = 1 - \frac{Mass\ \ of\ \ beads}{density\ \ of\ \ glass\ \ beads \times bed\ \ volume} \qquad \text{(eq 27)}$$

The air supply was opened and the liquid in the feed tank was saturated with oxygen. The column was pre-wetted, using either the Levec or Kan-liquid wetting procedure. Liquid and gas flow rates were selected to cover most of the trickle flow regime as this is where most industrial reactors operate. The data obtained in the experiments can be compared to most previous studies as these were done in the same operating range. Dissolution experiments were done using liquid velocities of 2, 3, 4, 5 and 8mm/s and a gas flow rate of 30mm/s. The electrochemical method was employed at superficial liquid velocities of 2, 3, 4 and 5mm/s were chosen and a gas flow rate of 30mm/s. The density of the electrolyte made experimenting at a liquid velocity of 8mm/s impractical as this flow rate is at the trickle-pulse flow transition boundary. One experiment was done, using each of the methods, for a gas flow rate of 60mm/s to investigate whether or not this greatly influences the solid-liquid mass transfer coefficients.

In Levec pre-wetting the gas flow rate is set at the desired value of 30mm/s, once the liquid is set at the desired flow rate the pressure release valve (V-2) is opened and the bottom of the column is sealed. The column is flooded from the bottom, this ensures that no air bubbles are trapped inside the column and that all the particles are completely wetted. Once the column is completely flooded the liquid flow is switched off, the pressure release valve is closed and the seal at the bottom of the column is removed thereby allowing the liquid to drain from the column. Liquid flow is only reintroduced once the mass in the column (residual liquid hold-up) remained constant for approximately five minutes. Pressure drop, dissolved oxygen concentration in the effluent and solid-liquid mass transfer measurements were either taken 5min, for electrochemical technique, or 10min, for the dissolution technique, after the desired liquid flow rate was reached.

In Kan-liquid pre-wetting the gas flow rate is again set at the desired flow rate of 30mm/s and is allowed time to stabilise. The liquid flow rate is increased, from a

zero flow rate, to the point of pulsing and then further increased to a point where the entire bed length of the bed is operating in the pulse flow regime. The bed is operated in the pulsing regime for approximately 15 seconds; this ensures complete wetting of the bed. Once this point has been reached the flow rate is decreased to the desired set point. Flow patterns are allowed to stabilize for 10min after which pressure drop, dissolved oxygen concentration and solid-liquid mass transfer measurements were taken.

The gas-liquid mass transfer coefficient was determined using a technique similar to that used by Goto & Smith (1975). The oxygen in the saturated liquid is transferred to the gas phase; therefore the difference in dissolved oxygen concentration in the feed and effluent can be used to infer the gas-liquid mass transfer coefficients (eq 32). The saturated dissolved oxygen concentration at a specific temperature was calculated using equation 28 to 31. No experiments were started before the particular saturation concentration in the liquid feed was observed on the oxygen probe monitor.

$$C_P = C^* \times P\left(\frac{(1-P_W/P)(1-\theta P)}{(1-P_W)(1-\theta)}\right) \qquad \text{(eq 28)}$$

where P_W is the partial pressure of the water vapour at the specific temperature (as calculated by equation 29) and θ is a correlating variable calculated by equation 30.

$$\ln P_W = 11.8571 - \left(\frac{3840.70}{T}\right) - \left(\frac{216.961}{T^2}\right) \qquad \text{(eq 29)}$$

$$\theta = 0.000975 - \left(1.426\times10^{-5}t\right) + \left(6.436\times10^{-8}t^2\right) \qquad \text{(eq 30)}$$

$$t = T - 273 \qquad \text{(eq 31)}$$

In order to correctly quantify the volumetric mass transfer coefficient the end effects should be taken into account. These end effects were studied by Loudon

(2006), using the same equipment and set-up used in this study, therefore his data was used here.

Pressure drop and gas-liquid mass transfer data were used compared to the data published by Loudon, Van der Merwe & Nicol (2006) and verified that measurements were taken after flow pattern stabilisation. These results are shown in appendix A.

3.2 Electrochemical solid-liquid mass transfer measurements

The solvent, electrolyte and current carrier used in this study was chosen according to the criteria set out by Latifi (1988) and Hanratty & Campbell (1983). Distilled water was used as solvent and a mixture of potassium ferricyanide and potassium ferrocyanide were used as electrolyte. Sodium hydroxide was used as current carrier. This system has been used in numerous previous studies which simplified comparison of experimental data with suggested correlations.

The electrolytic reaction at the cathode was the reduction of ferricyanide ions to ferrocyanide ions, described by reaction 1 (rxn 1), it should be noted that the reverse reaction occurred at the anode.

$$Fe(CN)_6^{3-} + e^- \rightarrow Fe(CN)_6^{4-} \qquad \text{(rxn 1)}$$

Two systems were employed to measure the mass transfer coefficient. In system A three cathodes were placed at different axial positions, with the same radial position, in the bed. The role of the cathode was played by a nickel sphere with the same diameter as the inert glass packing. A wire was soldered into the whole drilled through the middle of the nickel particle. System B consisted of a multiple packing electrode. A 4cm section of the column packing was replaced with (approximately 6000) nickel spheres of diameter equal to that of the inert packing. The anode, for both of system A and B, was made by soldering an

electrical wire to the sieve, supporting the packing particles. The two electrochemical systems as well as the dissolution system are diagrammatically shown in figure 7.

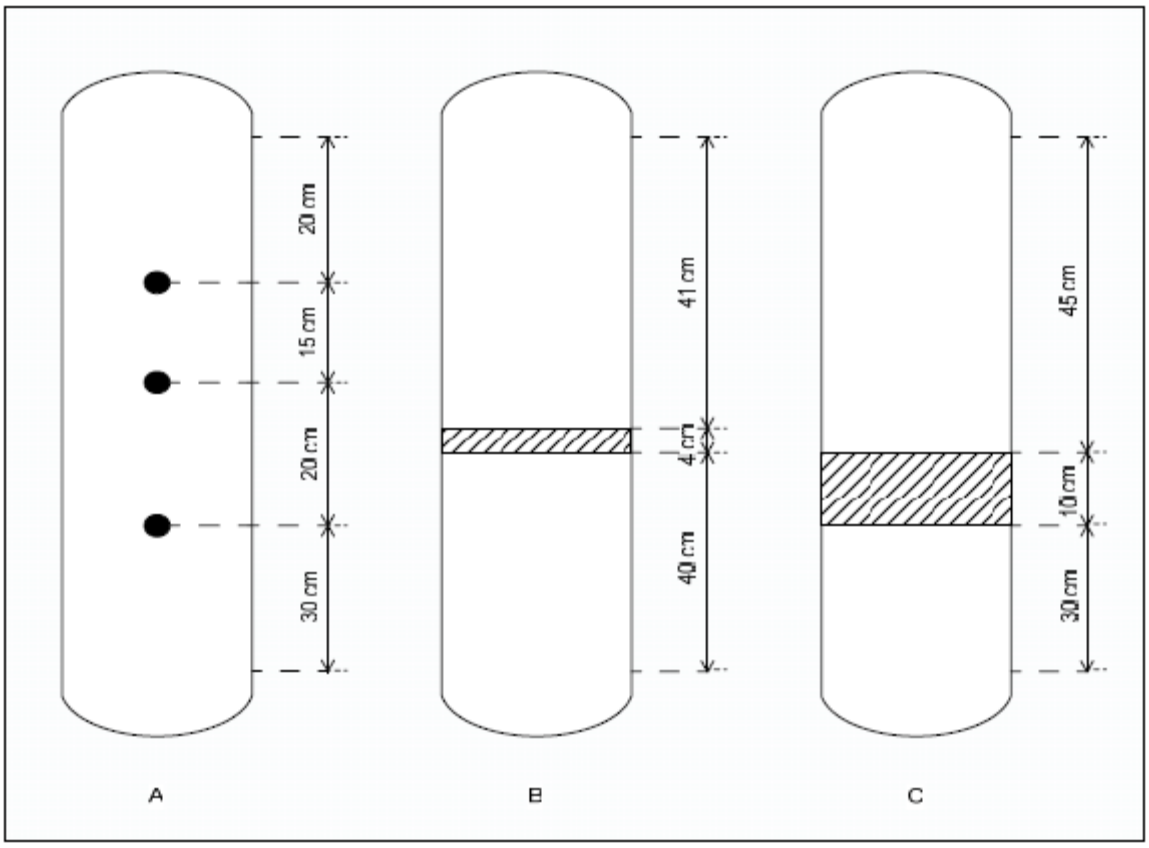

Figure 7: Electrode and active particle placement within the reactor: A) Single particle electrodes used in the electrochemical method, B) Multiple packing electrode for electrochemical method, C) Section of active particles for dissolution method

The diffusion plateau was determined in a randomly packed column. Glass spheres were loaded into the column inserting the cathode, either a single electrode or a multiple packing electrode, at the desired axial position. Single electrodes were placed 30, 50 and 65cm and the multiple packing electrode was placed 38cm from the supporting sieve. The distributor cap was mounted onto the top of the column and sealed. The column was then positioned on the stand (WT-1), the height and the mass of the packing was recorded for the determination of the bed density. Sutey & Knudsen (1976) noted that chemical polarisation of the electrode may occur therefore the column was reloaded after each experiment and a new cathode was used.

The feed tank was filled with a solution of 0.02M potassium ferrocyanide ($K_4Fe(CN)_6$), 0.003M potassium ferricyanide ($K_3Fe(CN)_6$) and 1M of sodium hydroxide ($NaOH$), the physical properties of this liquid is shown in table 4. *This concentration of current carrier resulted in a diffusion plateau at a voltage independent of the concentration of the electrolyte*. The liquid in the feed tank was pre-saturated with oxygen and the concentration of the dissolved oxygen noted. The temperature difference in the liquid feed was kept to a minimum (±2°C) so that saturation concentration of the dissolved oxygen was not affected. Once the feed was saturated the bed was wetted using the desired pre-wetting procedure. All experiments were done operating in the Levec and Kan-liquid modes.

Table 4: Physical properties of the electrolyte

Property	**Value**	**Units**
Density	1200	kg/m^3
Viscosity	1.02E-03	Poise
Diffusion coefficient	5.50E-09	m^2/s

The cathode was connected to the negative pole and the anode to the positive pole of a voltage source. The liquid flow rate was set at the desired set point and the voltage source switched on at 600mV, the current flow at this voltage was recorded. The voltage was incrementally increased to 1800mV, the current at these voltages were also recorded. This procedure was repeated for three liquid flow rates. Figure 8 shows the diffusion plateau reached for a single electrode at a bed height of 65cm. From this it is clear that a voltage of 1000mV will result in a diffusion limited reaction and therefore all the mass transfer coefficients were determined from limiting currents measured at 1000mV.

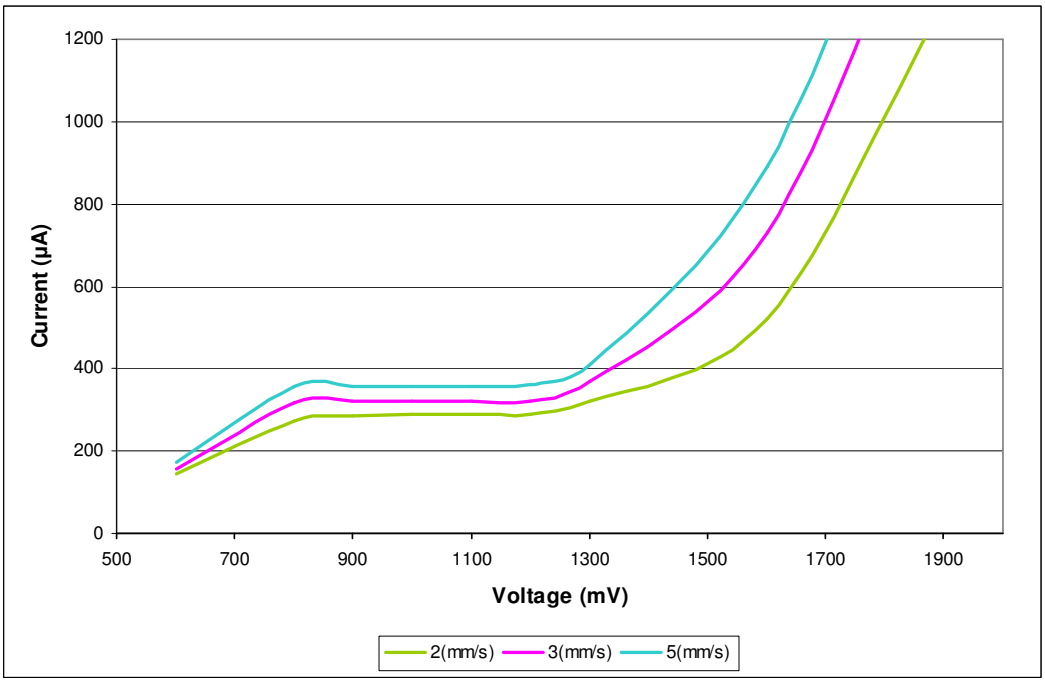

Figure 8: Diffusion plateau for an electrode placed at a bed height of 65cm

The experimental setup used and pre-experimental procedure, followed to obtain the diffusion plateau were also used to obtain limiting current measurements under trickle flow conditions. Gas and liquid were co-currently fed to the top of the column. The experimental procedure that followed after proper pre-wetting of the bed was as follows: The gas flow rate was kept constant at 30mm/s while the liquid flow rate was increased from 2mm/s to 5mm/s. The liquid flow rate was allowed to stabilise, for 5min, before the current flowing through the electrolyte, at 1000mV, was measured and recorded. The solid-liquid mass transfer coefficients were calculated using the equation developed by Hanratty & Campbell (1983).

$$I_{\lim} = Fk_{ls}A_eC \qquad \text{(eq 32)}$$

For initial calculations the area of the electrode was not separated from the mass transfer coefficient as the wetting efficiency was not known (Chapter 4). For further interpretation of the experimental results the wetting efficiency was assumed to be equal to that obtained by Van Houwelingen, Sandrock & Nicol (2006) (Chapter 5).

3.3 Dissolution solid-liquid mass transfer measurements

Two systems previously used in dissolution studies, benzoic acid and naphthalene, were considered for these experiments. Previous researchers reported difficulties in measuring the concentration of naphthalene in the effluent as some of the dissolved material was transferred to the gas phase. Another drawback reported in previous studies was the use of particles only made from the dissolving material. This complicated the hydrodynamics as the geometry of the particles and the bed height changes with time as the material dissolves. It was subsequently decided that benzoic acid was the best chemical to use as this will stay dissolved in the liquid and provide more accurate experimental results. Kernel spheres, 3mm glass beads, were coated with molten benzoic acid to ensure that the bed height and geometry stayed constant.

For this method the column was divided into three subsections. The first was a 30cm section at the bottom of the column packed with 3mm glass spheres. The second was a 10cm section filled with active particles, 3mm glass spheres coated with benzoic acid. The column was then filled, up to 85cm, with another section of glass beads. Once the column was loaded the distributor cap was mounted onto the top and the column was sealed. It was then positioned on the load cell (WT-1) and the height and the mass of the packing recorded for the determination of the bed density. The column was repacked, with freshly coated kernel spheres, after each experimental run.

The feed tank was filled with distilled water and saturated with oxygen. The packing was wetted using the desired pre-wetting procedure. Experiments were done using the Levec and Kan-liquid wetting procedures. Gas and liquid were co-currently fed to the top of the packed bed. The gas flow rate was kept constant at 30mm/s while the liquid flow rate was varied from 2mm/s to 8mm/s. The flow rates investigated are shown in table 6 below. The liquid flow rate was allowed to stabilise, for 15min, after which a sample of the effluent was taken. The effluent is titrated using a 0.0026M solution of $NaOH$. The concentration of benzoic acid was

calculated using equation 33. Using this concentration the solid-liquid mass transfer coefficient was determined by substitution in equation 3, repeated here for clarity. The properties of the effluent are given in table 5.

$$c_e = \frac{(Volume\ \ of\ \ titrating\ \ solution)(Concentration\ \ of\ \ titrating\ \ solution)}{Volume\ \ off\ \ effluent\ \ titrated} \qquad \text{(eq 33)}$$

$$k_{ls}a = \frac{U_L}{a_S h}\ln\left[\frac{c_S - c_f}{c_S - c_e}\right] \qquad \text{(eq 3)}$$

Table 5: Properties of the effluent

Property	**Value**	**Units**
Density	1000	kg/m^3
Viscosity	1.9 E-03	Poise
Diffusion coefficient	1.0E-09	m^2/s

3.4 Experimental repeatability

Previous studies reported that experimental repeatability in packed beds is hard or almost impossible to achieve. It was for this reason that all experiments were repeated three times for each flow rate and each electrode position. Figure 9 and 10 show the experimental repeatability achieved. The standard relative error of the electrochemical experimental data was 2.3% for operation in the Levec mode and 2.6% for operation in the Kan-liquid mode. The standard relative error for the experimental data obtained with the dissolution technique was 2.2% for operation in the Levec mode and 1.9% for Kan-liquid operation.

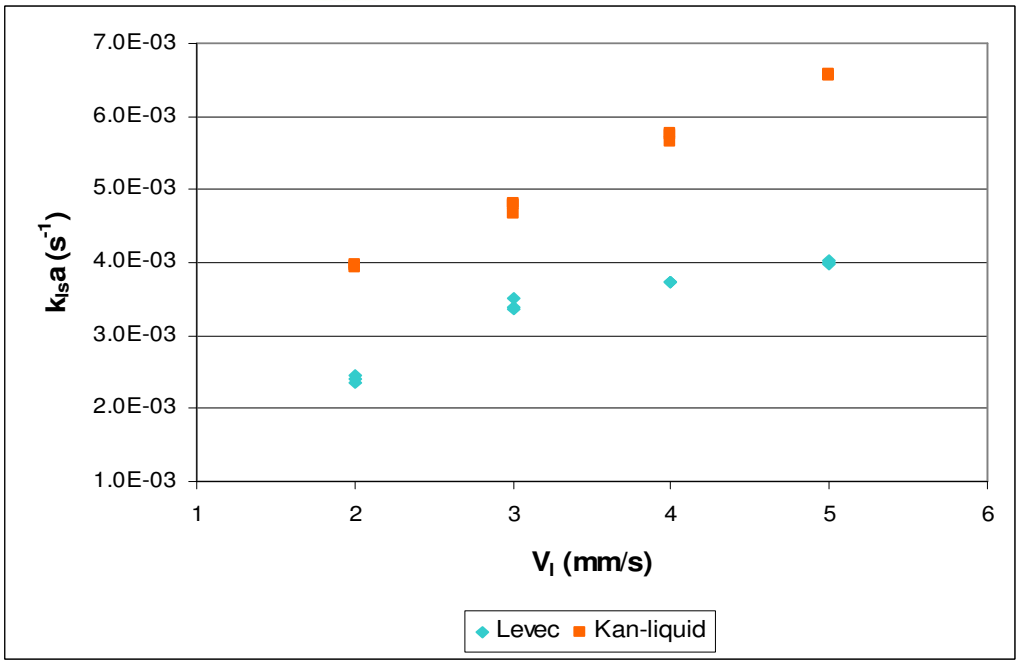

Figure 9: All experimental data obtained with the electrochemical method for a single electrode placed 30cm from the outlet. It should be noted that all flow rates in each operating mode was repeated three times and the entire data set obtained is shown here.

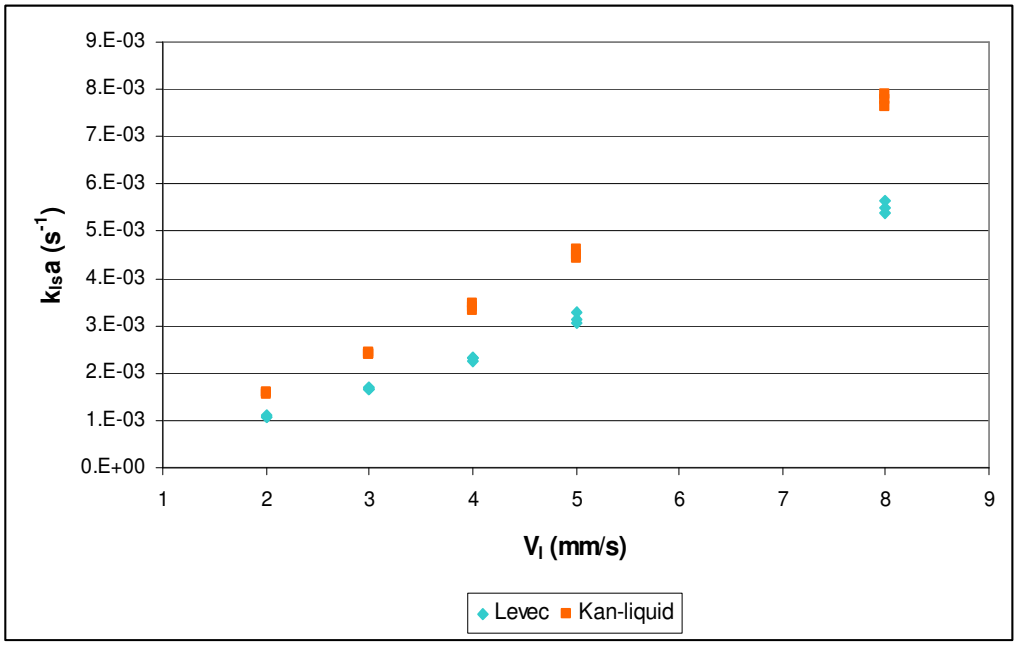

Figure 10: All experimental data obtained with the dissolution method. It should be noted that all flow rates in each operating mode was repeated three times and the entire data set obtained is shown here.

Chapter 4. Analysis of Measuring Techniques

Five data sets (one set dissolution, three single electrodes placed at different axial positions, and one set multiple packing electrode) each consisting of ten measurements (taken at five different liquid velocities in the Kan-liquid and Levec operating modes) were obtained. As expected the solid-liquid mass transfer coefficients measured at the top of the column was greater than that measured in the middle and the bottom of the column (discussed in section 5.2); therefore only the three data sets obtained from measurements in the middle of the column (dissolution, one single electrode, and a multiple packing electrode) were compared to one another. The experimental data of these three sets were also compared to previously suggested correlations.

4.1 Comparing single electrode and multiple packing electrode measurements

The significance of spatial variability of local mass transfer rates due to voidage non-uniformity and unstable liquid flow in the trickle flow regime has been widely recognised. Trivizadakis and Karabelas (2006) attributed the large spread in local Sherwood numbers, covering almost two orders of magnitude for a fixed pair of gas and liquid flow rates, to the aforementioned local packing variability and non-uniform liquid distribution. It is for this reason that one would expect a great variance of the mass transfer coefficients measured using a single electrode when compared to that measured with the multiple packing electrode, which should give a smaller spread of data and a better representation of mass transfer at the specific axial position.

Figure 11 shows the experimental data obtained with a single electrode, placed at a height of 30cm from the outlet, and a multiple packing electrode, at a height of 40cm from the outlet. It should be mentioned that all the data points and not

just average values were plotted. The average variance for measurements in the Levec mode was 3.3% and 7.8% for measurements in the Kan-liquid mode.

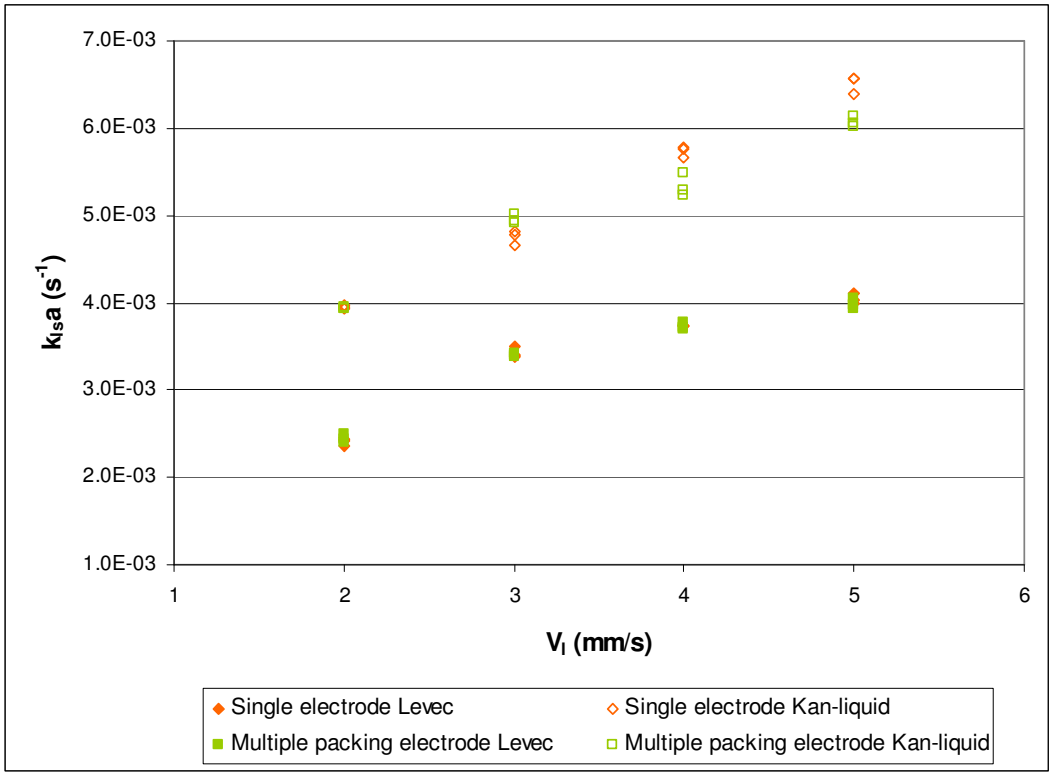

Figure 11: Solid-liquid mass transfer coefficients measured in the Levec and Kan-Liquid operating modes (Single electrode measurements at 30cm from outlet and multiple packing electrode at 40cm from the outlet)

Since the experimental data in figure 11 were obtained at different axial positions, mass transfer measurements for a single and a multiple packing electrode at the same axial position were taken and are shown in the parity plot below (figure 12). From these two figures it is clear that a single electrode gives an adequate representation of the overall mass transfer coefficient.

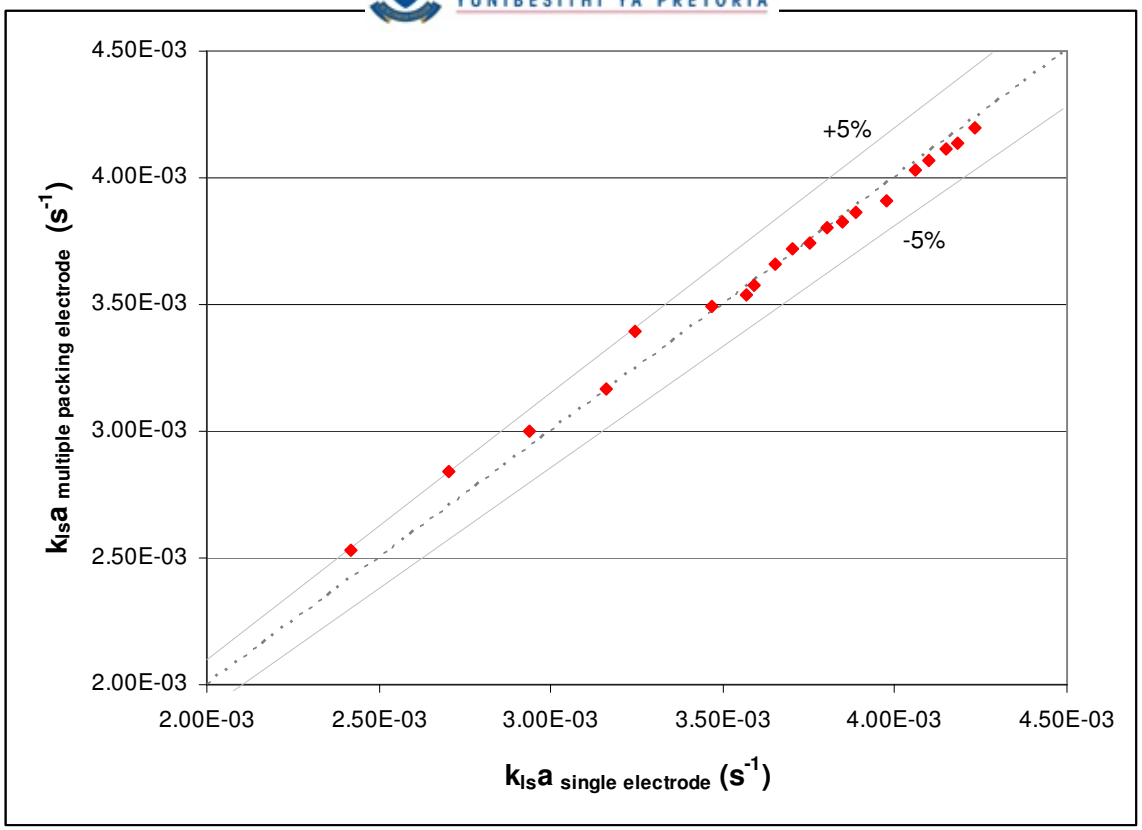

Figure 12: Mass transfer coefficients measured using a single electrode and a multiple packing electrode at the same bed height of 33cm from the outlet in a Levec pre-wetting mode

4.2 Comparing electrochemical and dissolution measurements

Figure 13 shows a comparison of the mass transfer coefficient data obtained with the electrochemical and dissolution techniques. For this comparison only the data obtained with the multiple packing electrode was used as it was in good agreement with that measured using a single electrode.

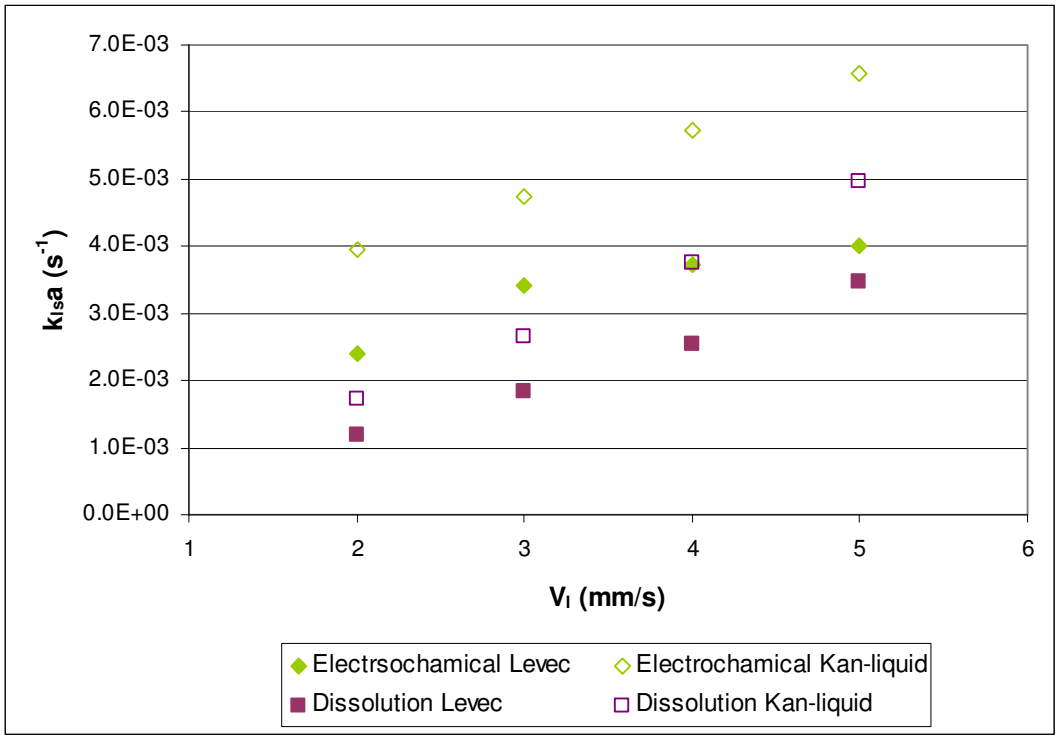

Figure 13: Comparison of experimental data obtained with a multiple packing electrode at 40cm from the outlet and the dissolution technique

The density and viscosity of the liquids used in the different techniques differ therefore figure 14 shows a comparison of the coefficients measured at the liquid Reynolds numbers. The correlation suggested by Lakota & Levec (1990), using a Kan-liquid pre-wetted bed and the dissolution of naphthalene particles, is higher than the dissolution data obtained in this study. The electrochemical data, based on the Kan-liquid mode of operation with a relatively low gas flow of 30mm/s, is in good agreement with the correlation suggested by Mochizuki (1974) even though this correlation was based on zero gas flow. When this is compared to previous studies shown in figure 3 (shown in Appendix C) it can be seen that the experimental data is on the lower end of the range of Sherwood numbers predicted by suggested correlation. *A comparison of data obtained with the dissolution method and the electrochemical method using single electrodes are shown in Appendix B.*

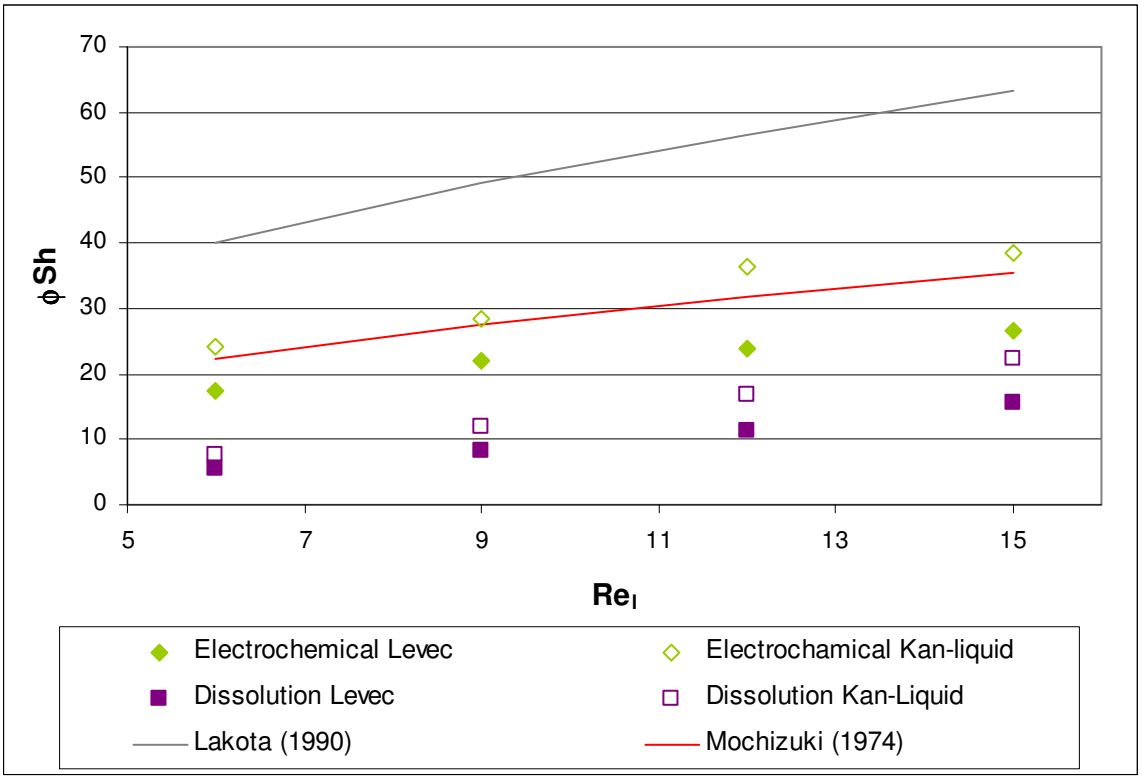

Figure 14: Mass transfer coefficients measured using a single electrode placed 50cm from the outlet and the dissolution method

Previously published data suggest that mass transfer coefficients measured using different techniques can lead to a large difference in the observed transfer coefficients. Two of these studies are Lakota & Levec (199) and Chou et al. (1979) where the Sherwood number predicted by the latter is 6.4 times higher. Such a variance in data was not observed in this study. This can be ascribed to the use of a single set of equipment, a multiple packing electrode, coating of a kernel sphere and the repacking of the column after each run. Measurements were also only taken once the liquid and gas flow stabilised.

Chapter 5. Hydrodynamic Results and Interpretation

5.1 Multiplicity results

Figure 15 shows the mass transfer coefficients obtained, with a single electrode placed 50cm above the outlet, with different liquid flow rates and using different pre-wetting procedures. The experimental data obtained in the Kan-liquid operating mode were as much as 1.6 times higher than the data in a Levec operated bed. Repeated experiments showed a variance of 2.4% in the Levec mode and 4.3% in the Kan-liquid mode. This is comparable to the variance for gas-liquid mass transfer coefficients (Appendix A) which have been shown to be repeatable for repacked beds.

It is evident that experimental data do not correlate with the proposal by Van der Merwe (2008) and that the Kan-liquid mode of operation out-performed the Levec mode in all the experiments. It does however coincide with the trend found by Sims et al. (1993) but differs in magnitude by a factor of 5.7. From the previous chapter it is clear that the dissolution data followed the same trend as the electrochemical data.

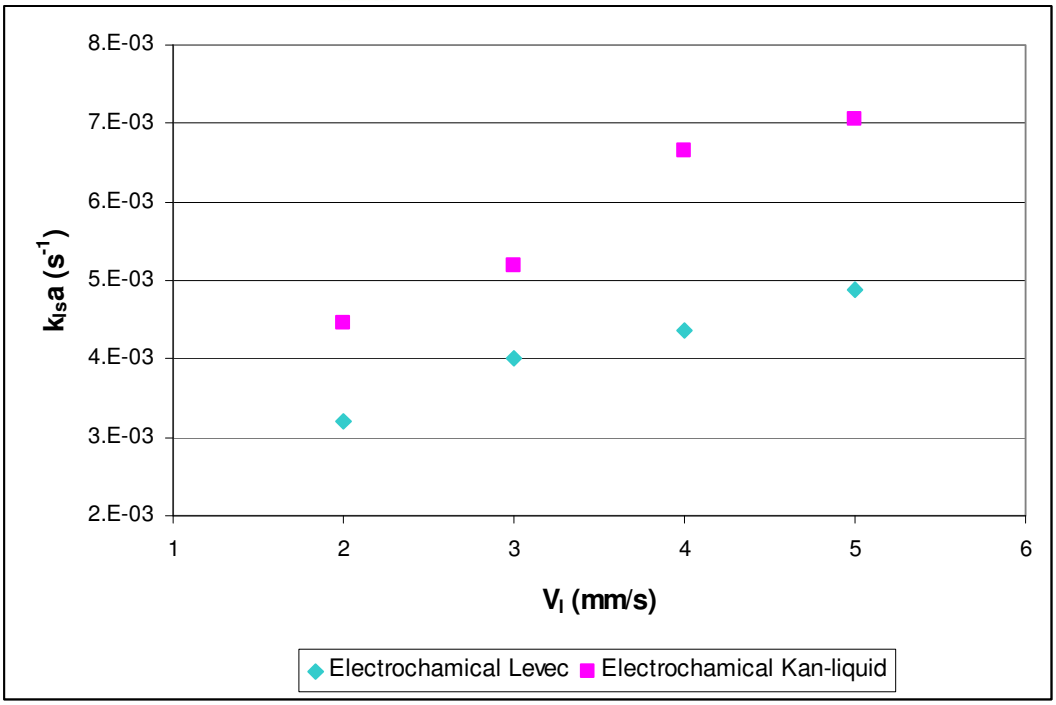

Figure 15: Average solid-liquid mass transfer coefficients measured 50cm from the outlet

Since LSMT is a function of hold-up and wetting efficiency, both which exhibit multiplicity, it was of interest to know how a change in these parameters affect the solid-liquid mass transfer coefficient and if it accounts for the multiplicity seen in figure 15. The liquid hold-up in the bed affects the average velocity experienced by the packing particles. This average flow over a particle is given by the intrinsic rate of liquid flow calculated using equation 34. As the Levec and Kan-liquid modes have different liquid hold-ups the interstitial velocity also differs. *The hold-up and wetting efficiency used are shown in table 6.*

$$u_{\text{int } rinsic} = \frac{V_l}{H} \qquad \text{(eq 34)}$$

Table 6: Wetting efficiency and hold-up measurements as taken from Van Houwelingen (2006) and Loudon (2006)

V_l (mm/s)	Wetting efficiency		Hold-up	
	Levec	Kan-liquid	Levec	Kan-liquid
2	0.58	0.71	0.060	0.123
3	0.62	0.73	0.085	0.147
4	0.64	0.76	0.097	0.153
5	0.70	0.81	0.106	0.161

Figure 16 shows the specific mass transfer coefficients (corrected for fractional surface area wetted) obtained with the electrochemical technique. The specific LSMT coefficients (m/s) measured in the Kan-liquid mode was higher than in the Levec mode even though the intrinsic liquid flow rate was lower. If the wetting efficiency and hold-up accounted for the multiplicity behaviour the specific mass transfer coefficients should lie in a single line, increasing with an increase interstitial velocity. It can therefore be deduced that these parameters cannot fully account for the multiplicity. The remaining difference can be explained by a faster refresh rate, i.e. less stagnancy, in the Kan-liquid mode. This is in agreement with the capillary gate theory posed by Van der Merwe (2009) which suggests that blocked pore necks causes some pores to be permanently filled with liquid and have no flow through them.

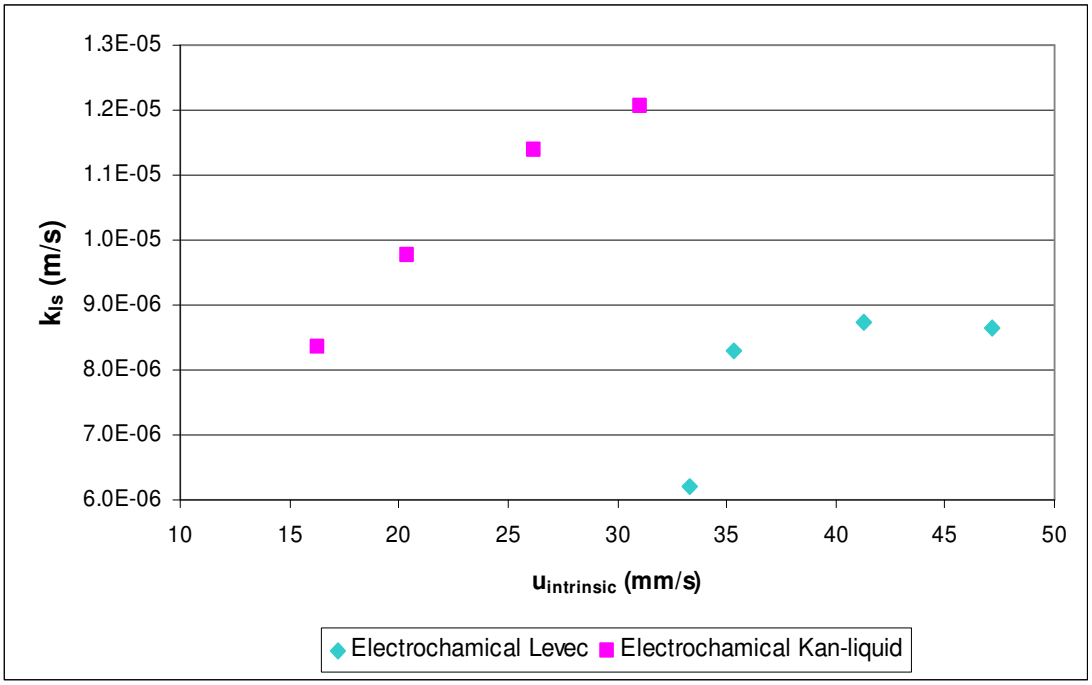

Figure 16: Solid-liquid mass transfer coefficient measured using the electrochemical method with an electrode placed 30cm from the outlet. Analysis of data for electrodes at different axial positions is shown in Appendix C.

5.2 Solid-liquid mass transfer as a function of bed height

The mass transfer coefficient measured at different bed heights are shown in figure 17 and 18. From this it is clear that the experimental data coincide with the findings by Trivizidakis & Karabelas (2006) that the mass transfer coefficient is smaller further down the bed. The measurements taken close to top of the column (65cm from the outlet) were up to 1.4 times higher that measured in the bottom in the bed (30cm from the outlet). If the data is examined closely it can be seen that the mass transfer coefficient measured at the top of the bed in the Levec mode is slightly lower than that measured at the bottom of the bed in the Kan-liquid operating mode. The exact mechanism as to what cause the drop in mass transfer is unclear. This is most probably due to a gradual alteration in the flow structure, but more research is needed to quantify this proposal.

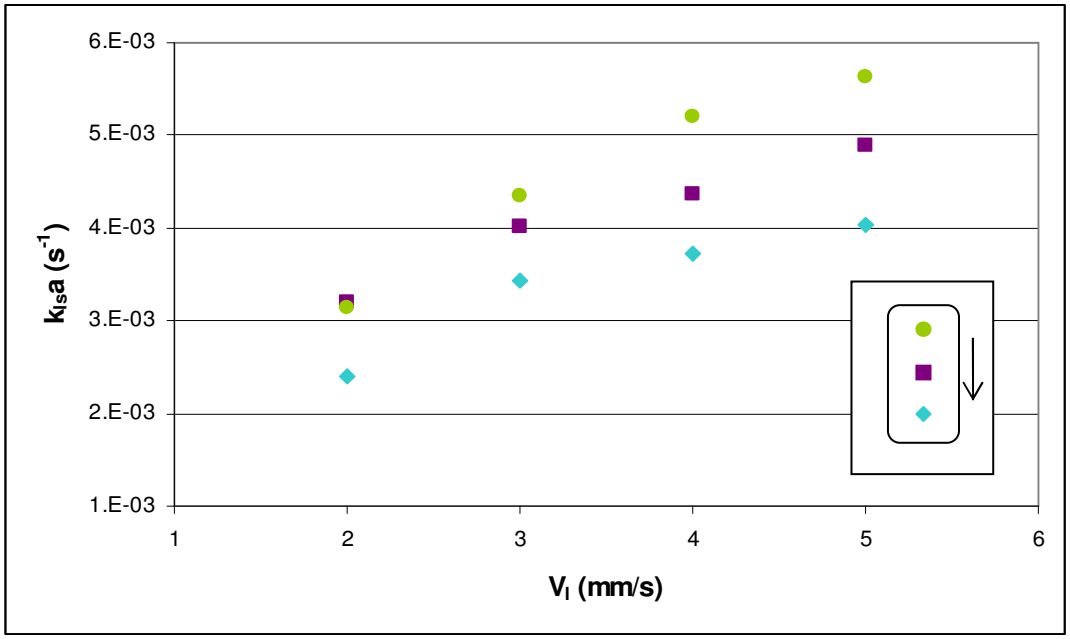

Figure 17: Solid liquid mass transfer coefficients at different bed heights for a Levec pre-wetted bed

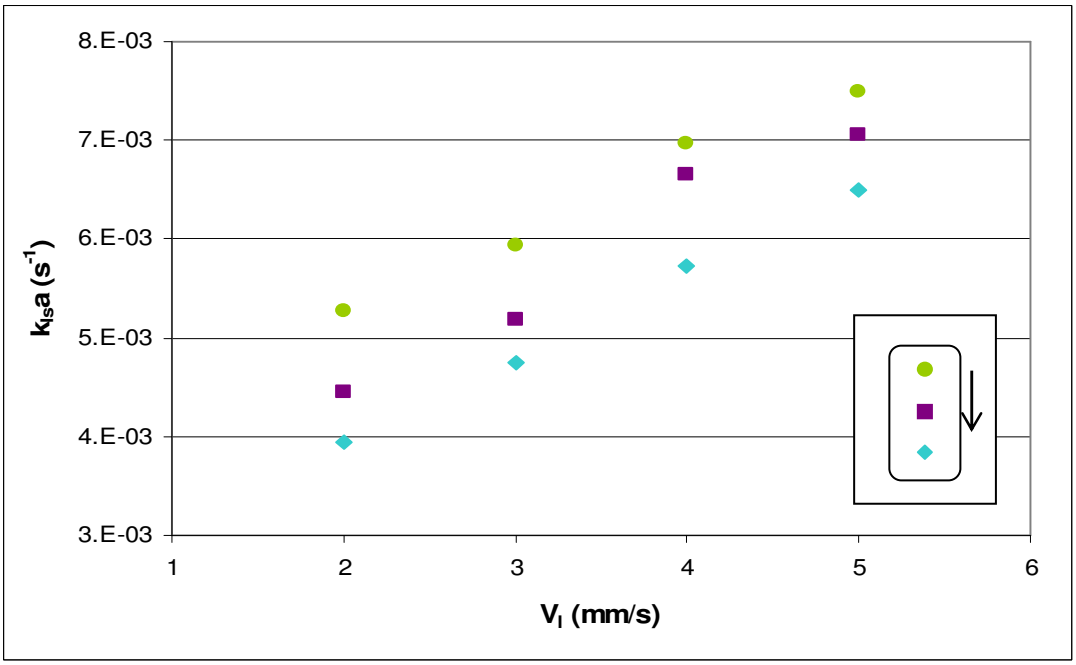

Figure 18: Solid liquid mass transfer coefficients at different bed heights for a Kan-liquid pre-wetted bed

Chapter 6. Conclusions

From this study it can be concluded that the volumetric solid liquid mass transfer coefficient exhibit significant multiplicity behaviour. The different pre-wetting procedures resulted in two distinct operating regions corresponding to the Levec and Kan-liquid operating modes. Mass transfer coefficients measured in the Kan-liquid operating mode were in the order of 1.6 times higher than those measured in the Levec operating mode. This agrees with the trend predicted by Sims et al. (1993) however the measurements are significantly lower than his experimental data. The speculation by Van der Merwe (2008) that a higher intrinsic liquid flow will lead to a higher mass transfer coefficient, in the Levec mode, was not observed. The difference in volumetric LSMT coefficients, in the Kan-liquid and Levec mode, cannot be explained by merely adjusting for the difference in wetting efficiency and hold-up. This is most likely due to a higher percentage of stagnant or poorly irrigated zones in the Levec mode, which is in agreement with the capillary gate theory (Van der Merwe, 2009) that suggests that blocked pores are filled with liquid and have no flow through them.

The two electrochemical methods, single electrode and multiple packing electrode, rendered similar mass transfer coefficients when measured at the same bed height. This implies that LSMT coefficients measured with a single electrode gives an adequate representation of a group of particles. Both the electrochemical and dissolution liquid-solid mass transfer measurements show a similar dependence on liquid flow rate. Measurements taken with the electrochemical method were on average 55% higher than those obtained with the dissolution method.

Lastly it was shown that mass transfer coefficients measured at the top of the column (65cm from the outlet) in a Levec operated bed were up to 1.4 times higher than that measured in the bottom of the column (30cm from the outlet) and 1.3 times higher in the Kan-liquid operating mode. This suggests that liquid flow structure changes with height.

References

Al-Dahhan, M. H., Larachi, F., Dudukovic, M. P., Laurent, A. (1997) "High-pressure trickle-bed reactors: A review" *Industrial Engineering Chemistry Research, 36,* 3292-3314

Al-Dahhan, M., High-Fill, W., Tee Ong, B. (2000) "Drawbacks of the dissolution method for measurement of the liquid-solid mass-transfer coefficient in two-phase flow packed bed reactors operated at low and high pressures" *Ind. Eng. Sci. Res., 39,* 3102-3107

Bartelmus, G. (1989) "Local liquid-solid mass transfer coefficients in a three-phase fixed bed reactor" *Chem. Eng. Process*, 26, 111-120

Barthole, G. (1982) *PhD thesis ,*INPL. Nancy

Burghardt, A., Bartelmus, G., Jaroszynski, M., Kolodziej, A. (1995) "Hydrodynamics and mass transfer in a three phase fixed-bed reactor with co-current gas-liquid down-flow" *the Chem. Eng. J., 58,* 83-99

Boelhouwer, J.G. (2001) "Nonsteady operation of trickle bed reactors: Hydrodynamics, mass and heat transfer" *PhD thesis*, Technical University Eindhoven

Chou, T. S., Worley, F. L., Luss, D. (1979) "local particle-liquid mass transfer fluctuations in mixed phase co-current down-flow through a fixed bed in the pulsing regime" *Ind. Eng. Chem. Fundam., 18 (3),* 279-283

Colombo, A.J., Baldi, G., Sicardi, S. (1976) "Solid-liquid contacting effectiveness in trickle bed reactors" *Chem. Eng. Sci.,* 31, 1101-1108

Delaunay, C. B., Storck, A., Laurent, A., Charpentier, J. C. (1982) "Electrochemical determination of liquid-solid mass transfer in a fixed-bed irrigated gas-liquid reactor with downward co-current flow" *Int. Chem Eng., 22 (2),* 244-251

Dharwadkar, A., Sylvester, N. D. (1977) “Solid-liquid mass transfer in packed beds” *AIChE Journal, 23 (3),* 376-378

Gianetto, A., Baldi, G., Specchia, V., Sicardi, S. (1978) “Hydrodynamics and solid-liquid contacting effectiveness in trickle-bed reactors” *AIChE Journal, 24 (6),* 1087-1104

Goto, S., Smith, J. M. (1975) “Trickle-bed reactor performance. Part I. Hold-up and mass transfer effects” *AIChE J., 21,* 706-713

Goto, S., Levec, J., Smith, J. M. (1975) “Mass transfer in packed beds with two-phase flow” *Ind. Eng. Chem., Process Des. Dev., 14 (4),* 473-478

Hanratty, T. J., Campbell, J. A. “Measurement of wall shear stress” in Goldstein, R. J., (1983) *Fluid Mechanics Measurements,* Hemisphere Publishing Corporation

Herskowitz, M., Carbonell, R.G., Smith, J.M. (1979) “Effectiveness factor and mass transfer on trickle bed reactors” *AIChE Journal, 25 (2), 272-283*

Hirose, T., Mori, Y., Sato, Y. (1976) “Liquid to particle mass transfer in fixed-bed reactors with co-current gas-liquid down-flow” *J. Chem. Eng. Japan, 9,* 220-225

Jolls, K. R., Hanratty, T. J. (1969) “Use of electrochemical techniques to study mass transfer rates and local skin friction to a sphere in a dumped bed” *AIChE Journal, 15 (2),* 199-205

Lakota, A., Levec, J. (1990) ““Solid-liquid mass transfer in packed beds with co-current downward two-phase flow” *AIChE Journal, 36 (9),* 1444-1448

Latifi, M. A., Laurent, A., Storck, A. (1988) “Liquid-solid mass transfer in packed beds with downward co-current gas-liquid flow: An organic liquid phase with high Schmidt number” *The Chem. Eng. J., 38,* 47-58

Latifi, M. A., Naderifar, A., Midoux, N. (1997) “Experimental Investigation of the Liquid/Solid Mass Transfer at the Wall of a Trickle-Bed Reactor—Influence of Schmidt Number” *Chem Eng Sci, 52 (21,22),* 4005-4011

Lemay, Y., Pineault, G., Ruether, J. A. (1975) “Particle-liquid mass transfer in a three-phase fixed bed reactor with co-current flow in the pulsing regime” *Ind. Eng. Chem., Process. Des. Dev., 14 (3),* 280-285

Levec, J. Grosser, K., Carbonall, R.G. (1988) “The hysteretic behaviour of pressure drop and liquid hold-up in trickle bed reactors” *AIChE journal*, 34 (6), 1027-1030

Loudon, D. (2006) “The effect of pre-wetting on pressure drop, liquid hold-up and gas-liquid mass transfer in trickle bed reactors” *Masters dissertation*, University of Pretoria

Loudon, D., Van der Merwe, W., Nicol, W. (2006) “Multiple hydrodynamic states in trickle flow: Quantifying the extent of pressure drop, liquid holdup and gas–liquid mass transfer variation” *Chem. Eng. Sci.,* 26, 7551-7562

Maiti, R., Khanna, R., Nigam, K.D.P. (2006) “Hysteresis in trickle bed reactors: A review” *Ind. Eng. Chem. Res.*, 45 (15), 5185-5198

Mochizuki, S., Matsui, T. (1974) “Liquid-solid mass transfer rate in liquid-gas upward co-current flow in packed beds” *Chem. Eng. Sci., 29,* 1328

Mochizuki, S., Matsui, T. (1976) “Selective hydrogenation and mass transfer in a fixed bed catalytic reactor with gas-liquid co-current up-flow” *AIChE Journal, 22 (5),* 904-909

Morita, S., Smith, J. M. (1978) “Mass transfer and contacting efficiency in a trickle bed reactor” *Ind. Eng. Chem. Fundam., 17 (2),* 113-120

Rao, V. G., Drinkenburg, A. A. H. (1985) “Solid-liquid mass transfer in packed beds with co-current gas-liquid down flow” *AIChE Journal, 31 (7),* 1059-1068

Ruether, J. A., Yang, C., Hayduk, W. (1980) “Particle mass transfer during co-current downward gas-liquid flow in packed beds” *Ind. Eng. Chem. Proc. Des. Dev., 19,* 103-107

Satterfield, C. N., Resnick, N. (1954) ”Simultaneous heat and mass transfer in a diffusion-controlled chemical reaction. Part II. Studies in a packed bed.” *Chem. Eng. Prog., 50,* 504-510

Satterfield, C. N., Pelossof, A. A., Sherwood, T. K. (1969) “Mass transfer limitations in a trickle bed reactor” *AIChE Journal, 15 (2),* 226-234

Satterfield, C. N. (1975) “Trickle bed reactors” *AIChE Journal, 21 (2),* 209-228

Satterfield, C. N., Van Eek, M. W., Bliss, G. S. (1978) “Liquid-solid mass transfer in packed beds with downward co-current gas-liquid flow” *AIChE Journal, 24 (4),* 709-717

Sims, W., Schultz, F. G., Luss, D. (1993) “Solid-liquid mass transfer to hollow pellets in a trickle bed” *Ind. Eng. Chem. Res., 32,* 1895-1903

Specchia, V., Baldi, G., Gianetto, A. (1978) “Solid-liquid mass transfer in co-current two-phase flow through packed beds” *Ind. Chem. Eng. Process Des. Dev., 17,* 362

Sutey, A.M., Knudsen, J.G. (1976) “Effect of dissolved oxygen on the redox method for measurement of mass transfer coefficients” *I&EC Fundamentals, 6 (1),* 132-139

Sylvester, N. D., Pitayagulsarn, P. (1975) “Mass transfer for two-phase co-current down flow in a packed bed” *Ind. Eng. Chem. Proc. Des. Dev., 14 (3),* 421-426

Tan, C. S., Smith, J. M. (1982) “A dynamic method for liquid-particle mass transfer in trickle beds” *AIChE Journal, 28 (2),* 190-195

Tsochatzidis, N.A., Karabelas, A.J., Giakoumakis, D., Huff, G.A. (2002) "An investigation of liquid maldistribution in trickle beds" *Chem. Eng. Sci., 57,* 3543-3555

Trivizadakis, M. E., Karabelas, A. J. (2006) "A study of local liquid/solid mass transfer in packed beds under trickling and induced pulsing flow" *Chem. Eng. Sci., 61,* 7684-7696

Van der Merwe, W. (2004) "The morphology of trickle flow liquid hold-up" *Masters dissertation*, University of Pretoria

Van der Merwe, W., Nicol, W., Al-Dahhan, M.H. (2008) "Effect of hydrodynamic multiplicity on trickle bed reactor performance" *AIChE journal,* 54(1), 249-257

Van der Merwe, W. (2008) "Trickle flow hydrodynamic multiplicity" *PhD thesis,* University of Pretoria

Van Houwelingen, A. (2006) "The morphology of solid-liquid contacting efficiency in trickle flow" *Masters dissertation,* University of Pretoria

Van Houwelingen, A., Sandrock, C., Nicol, W. (2006) "Particle wetting distribution in trickle bed reactors" *AIChE*, 52 (10), 3532-3542

Van Krevelen, D. W., Krekels, J. T. C. (1948) *Recl. Trav. Chim., 67,* 512 quoted by Goto, S., Levec, J., Smith, J. M. (1975) "Mass transfer in packed beds with two-phase flow" *Ind. Eng. Chem., Process Des. Dev., 14 (4),* 473-478

Wilson, E.J., Geankoplis, C.J. (1966) "Liquid mass transfer at very low Reynolds numbers in packed beds" *I&EC fundamentals*, 5(1), 9-14

Appendix A

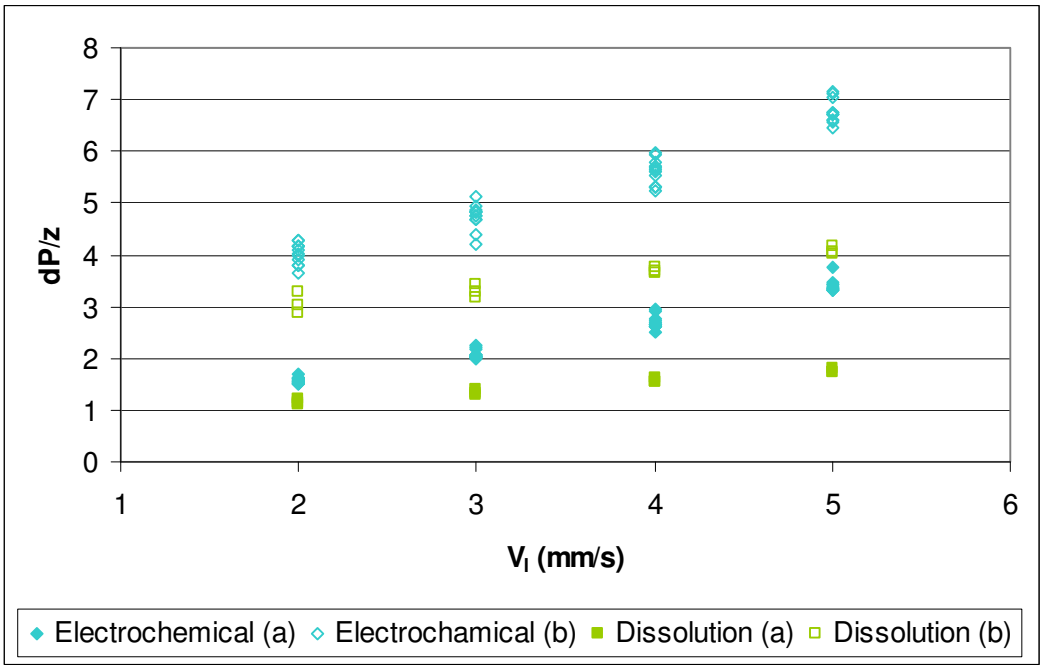

Figure 19: Pressure drop a)Levec pre-wetted bed b)Kan-Liquid pre-wetted bed (constant gas flow rate 30mm/s)

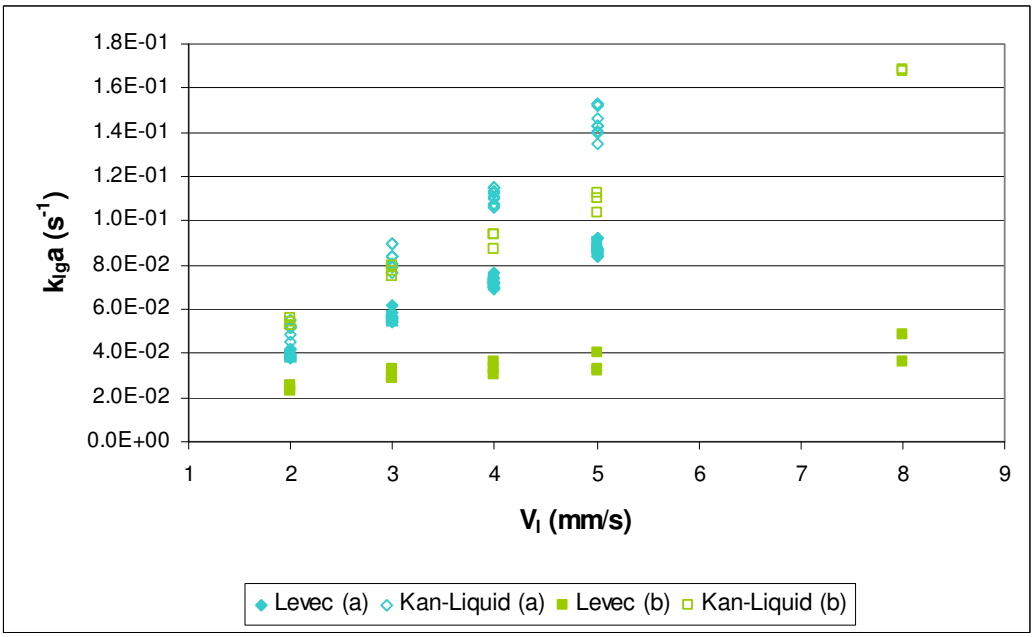

Figure 20: Hysteretic behaviour of the solid-liquid mass transfer coefficient (gas flow rate was kept constant at 30mm/s) a)Electrochemical method and b)Dissolution method

Appendix B

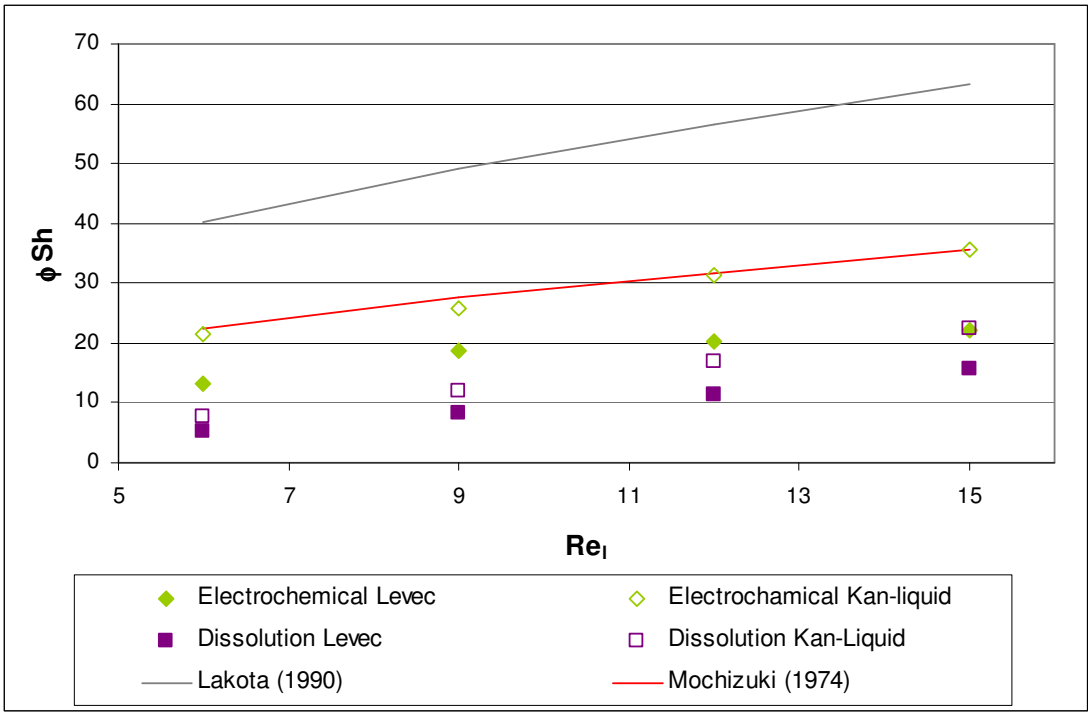

Figure 21: Mass transfer coefficients measured using the dissolution and the electrochemical method using a single electrode placed 30cm from the outlet

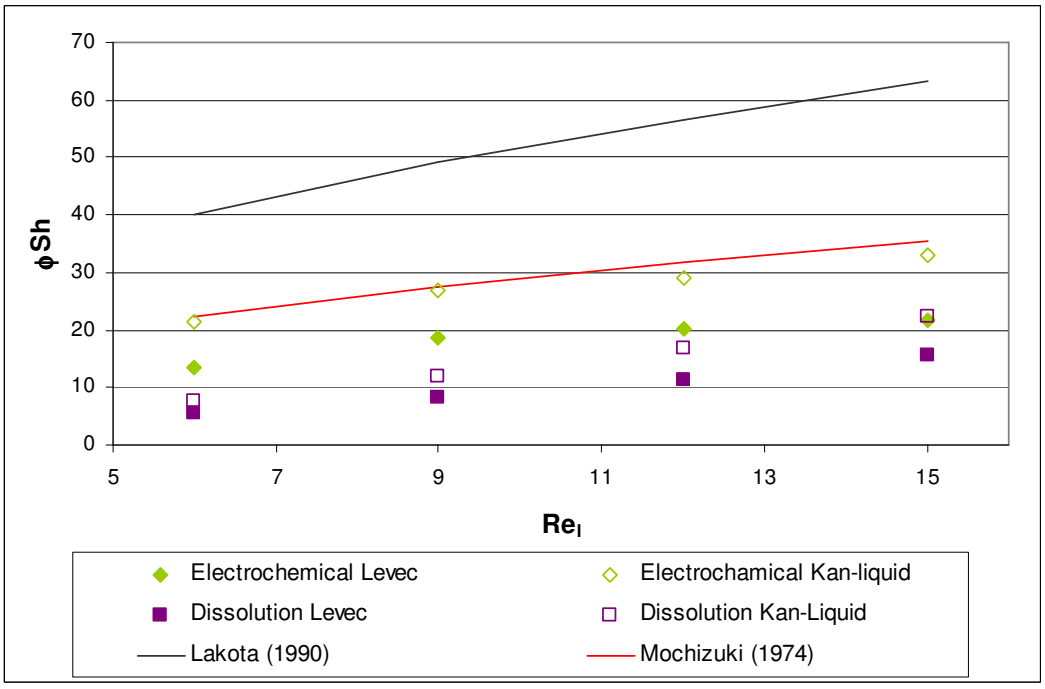

Figure 22: Mass transfer coefficients measured using the dissolution and the electrochemical method using a multiple packing electrode placed 40cm from the outlet

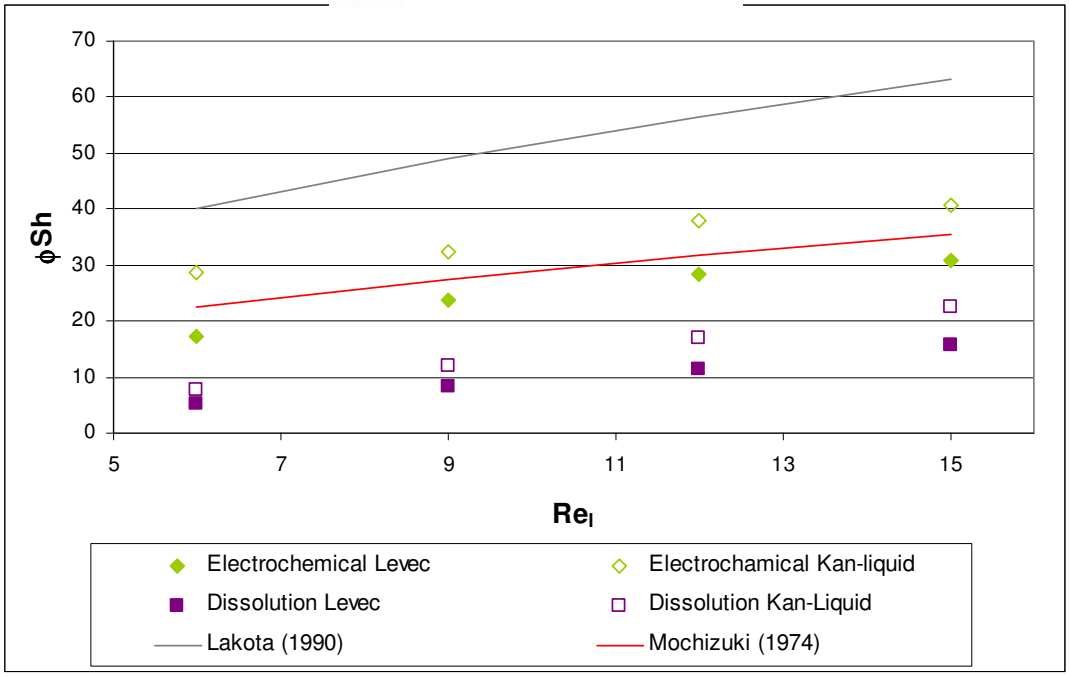

Figure 23: Mass transfer coefficients measured using the dissolution and the electrochemical method using a single electrode placed 65cm from the outlet

Appendix C

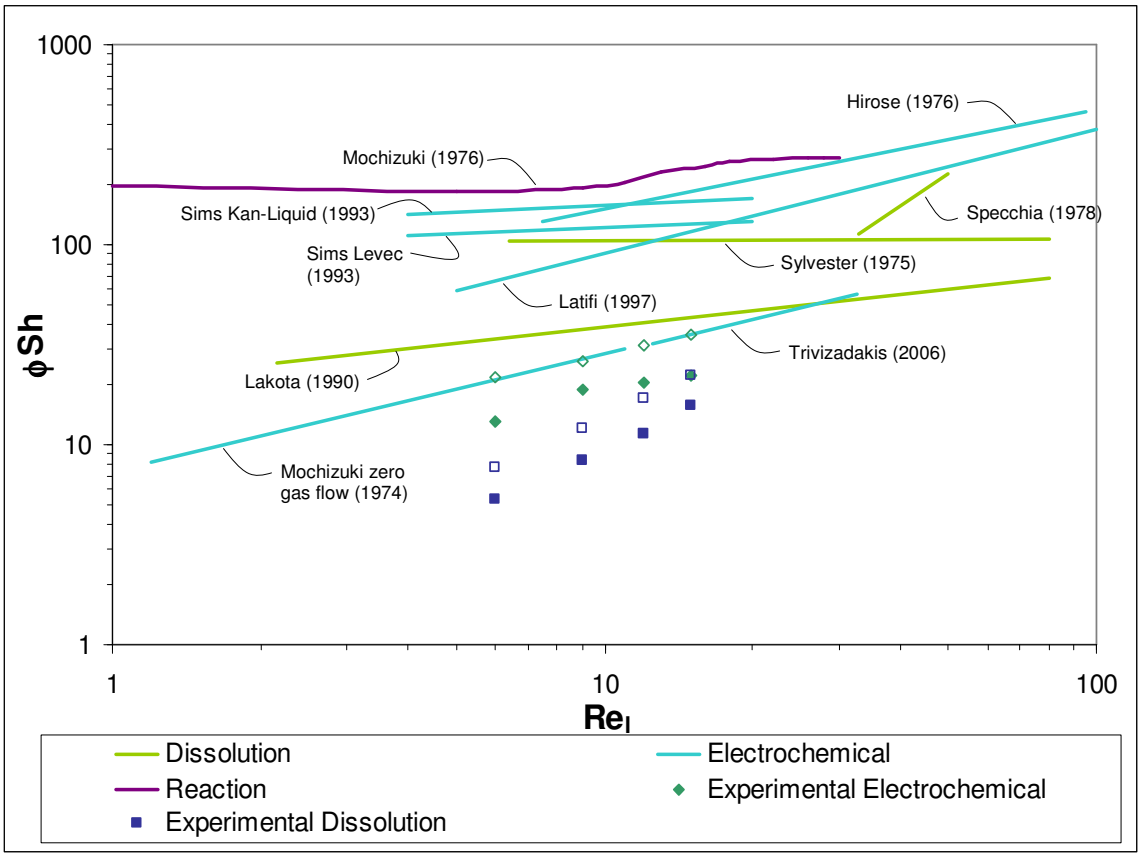

Figure 24: Comparison of experimental data with generally accepted solid-liquid mass transfer correlations

Appendix D

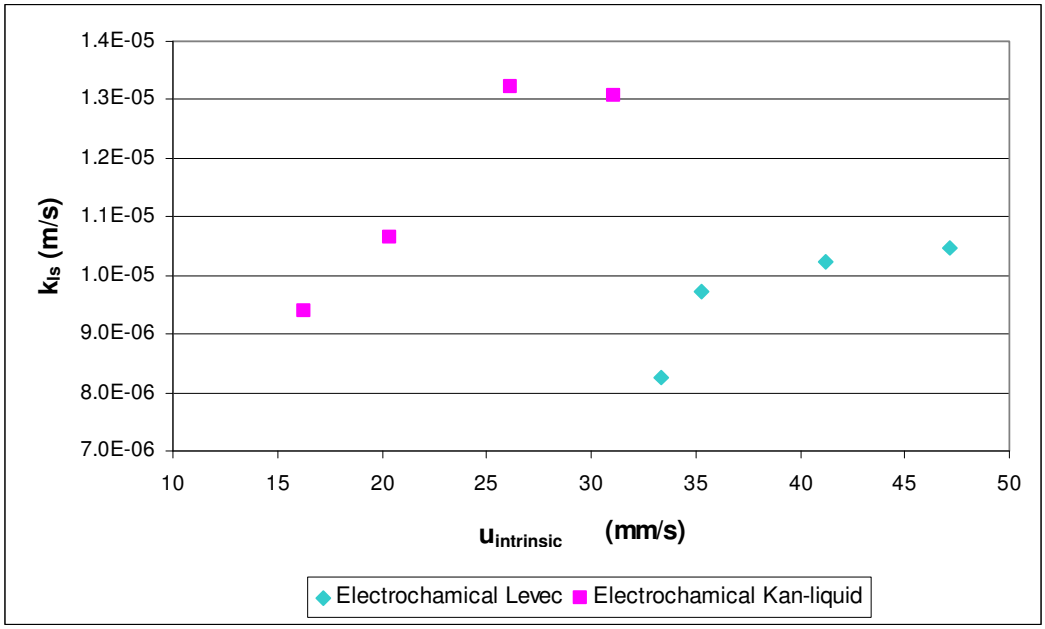

Figure 25: Solid-liquid mass transfer coefficient measured using a single electrode placed 50 cm from the outlet

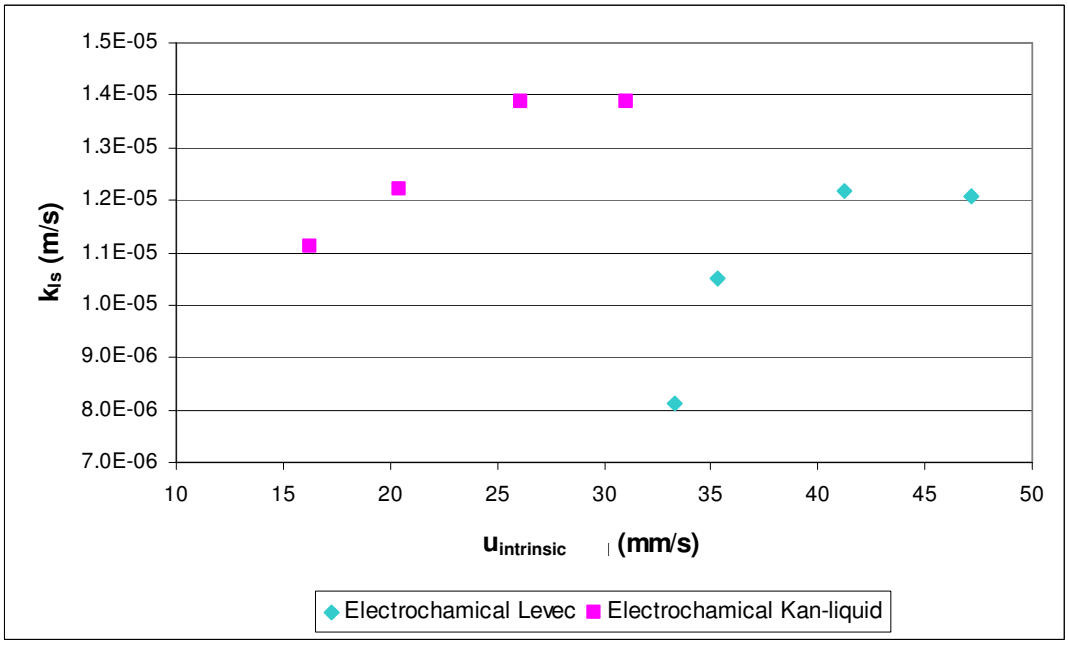

Figure 26: Solid-liquid mass transfer coefficient measured using a single electrode placed 65 cm from the outlet

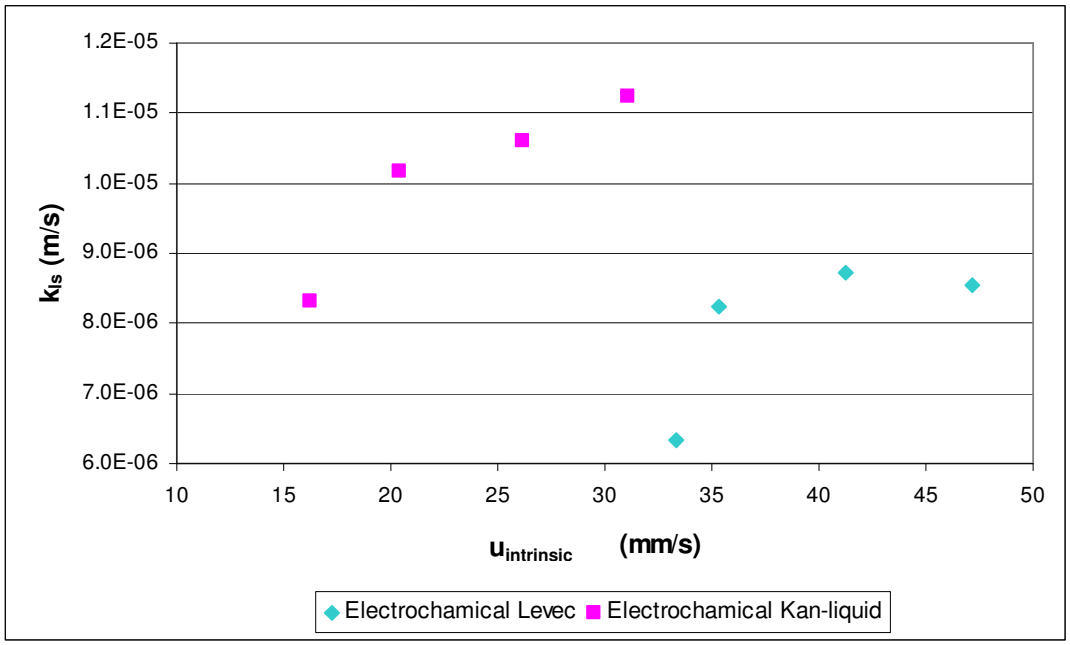

Figure 27: Solid-liquid mass transfer coefficient measured using a multiple packing electrode placed 44cm from the outlet